

Multiple double-valley and single-valley dark solitons in the complex modified Korteweg–de Vries equation: shape-preserving collisions and shape-altering collisions

Yingcan Huang¹, Jingsong He¹, T. Kanna², and Jiguang Rao³

¹*Institute for Advanced Study,
Shenzhen University, Shenzhen,
Guangdong 518060, P. R. China*

²*Nonlinear Waves Research Lab,
PG and Research Department of Physics, Bishop Heber College,
Tiruchirappalli - 620 017, Tamil Nadu, India*

³*School of Mathematics and Statistics,
Hubei University of Science and Technology,
Xianning, Hubei, 437300, P. R. China*

*

The shape-preserving and shape-altering collisions of general dark solitons are investigated in the complex modified Korteweg–de Vries equation. The obtained dark soliton solutions are classified into two distinct types, referred to as type-I and type-II dark solitons, which exhibit fundamentally different structural and dynamical characteristics. A single type-I dark soliton is symmetric about its center and admits three distinct valley profiles, namely single-valley, double-valley, and flat-bottom structures, whereas a single type-II dark soliton only supports a single-valley profile. These two types of dark solitons differ not only in their phase behaviors as the spatial variable varies from $-\infty$ to $+\infty$, but also in their velocity–amplitude relations. For multiple pure type-I dark solitons, collisions are shape-preserving; however, an unusual collective effect is revealed in which modifying the parameters of one soliton can induce changes in the profiles and amplitudes of the other solitons, even though all collisions remain elastic in nature. In contrast, multiple pure type-II dark solitons behave independently, undergoing only phase shifts without any modification of their shapes or amplitudes. When type-I and type-II dark solitons coexist, their interactions lead to genuinely shape-altering collisions, where the valley structures and amplitudes of type-I dark solitons are modified, while type-II solitons remain unaffected except for phase shifts. Through asymptotic analysis, it is further shown that the influence of type-II dark solitons on type-I dark solitons is confined to the pre-collision stage and disappears asymptotically after the interaction. These results reveal rich collision-induced dynamical behaviors of dark solitons in the complex modified Korteweg–de Vries equation and provide insights into nontrivial interaction mechanisms of localized nonlinear excitations.

* Email of corresponding authors:hejingsong@szu.edu.cn(J.He); kanna_phy@bhc.edu.in (T. Kanna)

I. INTRODUCTION

Solitons are fundamental to the study of nonlinear physics and are renowned for their remarkable ability to preserve both shape and velocity over long distances without dispersion [1]. In contrast to conventional waves, which typically broaden and attenuate during propagation, solitons exhibit particle-like behavior, maintaining localized and stable profiles through a precise balance between dispersion and nonlinearity in the medium [2]. This distinctive feature has attracted considerable attention because of its wide applicability across diverse technological contexts [3]. In particular, optical solitons have been extensively studied in fiber-optic communication systems, where they enable long-distance information transmission with minimal energy loss, offering a compelling solution to signal degradation [4]. Beyond telecommunications, solitons play important roles in fields such as fluid dynamics [5], plasma physics [6], and Bose-Einstein condensates (BECs) [7].

Bright and dark solitons represent two fundamental classes of solitonic structures, distinguished by their characteristic waveforms and diverse applications in nonlinear science [8]. Bright solitons manifest as intense, localized peaks in self-focusing media, where the wave energy is concentrated in a small region, producing a burst-like appearance [1]. In contrast, dark solitons appear as dips or voids in a continuous wave field, stabilized within self-defocusing media [9]. The formation of these solitons depends on the nature of the nonlinearity in their environment: bright solitons require self-focusing properties to maintain their integrity, while dark solitons arise from self-defocusing effects. These distinctions make each type of soliton influential across diverse scientific domains. Bright solitons, for example, are valuable in optical fiber networks, where their robustness supports efficient data transmission. Dark solitons, with their unique low-intensity profiles, contribute to advancements in photonics and atomic physics, where they are studied in phenomena like optical vortices. Apart from the obvious difference in the density of bright and dark solitons, the latter have distinctive dynamic properties. For instance, multi-component dark vector solitons typically undergo trivial interactions [10, 11], whereas bright vector solitons can exchange energy between components, leading to polarization changes [12, 13]. Their role in fluid dynamics and beyond highlights the solitons' wide-ranging influence, as they continue to inspire innovation and provide insights into fundamental wave behavior across various fields.

Solitons are intriguing mathematical entities that arise as solutions to specific integrable nonlinear evolution equations [14]. Their exceptional collision dynamics and various other characteristics have made them valuable in practical applications. One such crucial physical model is the complex modified Korteweg-de Vries (cmKdV) equation [15–17],

$$u_t + u_{xxx} + 6\gamma|u|^2u_x = 0, \quad (1)$$

which supports both bright and dark soliton solutions. Notably, the nonlinearity coefficient γ can be either positive or negative, depending on the physical context. For instance, in describing light propagation in liquid-crystal waveguides, this coefficient is positive [18]. Conversely, in deriving the cmKdV equation for strongly dispersive waves in a weakly nonlinear medium using a multiple-scale expansion (as shown in Ref. [18]), the nonlinear coefficient takes a negative value. This coefficient can typically be normalized to $\gamma = \pm 1$, where the case $\gamma = 1$ corresponds to bright solitons, while $\gamma = -1$ corresponds to dark solitons. For $\gamma = 1$, Eq. (1) reduces to the focusing complex modified Korteweg-de Vries (cmKdV) equation, which has been extensively studied through diverse analytical frameworks. The N -bright soliton solutions were systematically constructed via the Darboux transformation [19], while higher-order soliton solutions were investigated using both the inverse scattering method [20] and refined Darboux transformation techniques [21, 22]. Beyond fundamental soliton structures, breather solutions were derived in Darboux transformation framework [23], and rogue wave solutions were comprehensively analyzed using Darboux transformation methods [24–26] complemented by bilinear approaches [27]. Recent studies on the focusing cmKdV investigate the long-time asymptotics of localized solutions [28], the soliton-collision dynamics of the (2+1)-dimensional nonlocal complex mKdV system [29], and the large-order asymptotics of multi-rational solitons [30]. When $\gamma = -1$, Eq. (1) reduces to the defocusing cmKdV equation, where progress on dark soliton studies has been relatively limited. The fundamental single dark soliton solution was first established through Painlevé analysis and truncation methods [31], followed by the systematic derivation of N -dark soliton solutions via binary Darboux transformation [32]. Subsequent extensions to multi-component systems yielded dark vector soliton solutions through Darboux transformation methodologies [33, 34]. The Cauchy problem with step-like initial conditions was resolved through the Whitham modulation theory, as demonstrated in works by Kodama *et al.* [35] and subsequent refinements [36, 37]. In addition to classical approaches, improved bilinear formulations have yielded novel exact solutions for nonlocal variants of the cmKdV equation, broadening its solution space [38]. More recently, gradient-optimized physics-informed neural networks have emerged as efficient solvers, offering a flexible deep-learning framework to approximate nonlinear wave dynamics beyond traditional methods [39]. Notably, all reported dark solitons in the cmKdV equation exhibit shape-preserving collisions with single-valley profiles.

From a dynamical viewpoint, the robustness of soliton collisions is often regarded as a hallmark of integrable nonlinear wave systems. In this framework, dark solitons are commonly viewed as particle-like localized excitations whose interactions are purely elastic, characterized by the preservation of their shapes and amplitudes up to phase

shifts. This elastic-collision paradigm has been widely adopted in the study of dark solitons and underpins the conventional understanding of their stability and interaction properties. However, this picture is largely based on dark solitons with relatively simple internal structures. When more intricate internal degrees of freedom are involved, such as multi-valley profiles, it is not a priori clear whether the standard elastic-collision paradigm remains valid. In particular, it remains an open question whether collisions between such structurally rich dark solitons necessarily preserve their internal profiles, or whether interaction-induced structural transformations can occur even within an integrable setting. Addressing this issue is essential for elucidating how internal structures influence soliton interactions and for advancing the understanding of nonlinear wave dynamics beyond the conventional particle-like description.

This paper conducts an in-depth study of dark solitons in the cmKdV equation with $\gamma = -1$, namely,

$$u_t + u_{xxx} - 6|u|^2u_x = 0. \quad (2)$$

We demonstrate that both shape-preserving and shape-altering collisions of dark solitons occur in Eq. (2). In particular, the shape-preserving collisions of one specific type of dark soliton reveal novel solitonic behaviors, while shape-altering collisions are rarely reported in previous studies. Motivated by the dynamical issues discussed above, our investigation focuses on three main aspects. First, we systematically construct general dark soliton solutions of the cmKdV equation. This equation admits two types of dark solitons with distinct properties, which are classified as type-I and type-II dark solitons. The general solutions are obtained via the KP bilinear method [40–43], where the τ -function is expressed as the determinant of a block-structured matrix with four sub-blocks. Notably, the dimension of the first sub-block is twice the number of type-I solitons, whereas the dimension of the last sub-block equals the number of type-II solitons. The detailed derivations are provided in Appendix A. Second, we analyze the dynamics of the fundamental dark soliton solutions. Specifically, there exist precisely two types of fundamental solutions. To clarify their differences, we examine single-soliton solutions of each type in detail, focusing on velocity, amplitude, and profile. A key result is that the type-I dark soliton can exhibit three distinct profiles—double-valley, flat-bottom, and single-valley—depending on its velocity. The precise conditions for each profile are discussed in the paper. In contrast, the type-II soliton always maintains a single-valley profile regardless of velocity. To the best of our knowledge, type-I dark solitons that admit three distinct profiles have not been reported before in scalar integrable systems. Third, we investigate the collision dynamics of multi-soliton solutions. We first study collisions between two solitons, covering three cases: two type-I solitons, two type-II solitons, and mixed type-I and type-II solitons. Shape-altering collisions occur only in the mixed case, while the other two cases exhibit shape-preserving collisions. We then extend our analysis to collisions among arbitrary numbers of solitons in the cmKdV equation and derive the asymptotic forms of the solutions before and after collisions. The asymptotic analysis confirms that shape-altering collisions occur exclusively in mixed type-I and type-II cases. Specifically, a type-I soliton is influenced only by solitons of the same type before collision, but after collision, it is affected by both types. This mechanism accounts for the inelastic nature of mixed collisions.

The remainder of the paper is organized as follows. Section II presents explicit formulas for the general dark soliton solutions and analyzes the dynamics of the two types of single solitons. Section III investigates collisions between two solitons in the three basic cases (pure type-I, pure type-II, and mixed). Section IV extends the analysis to collisions among arbitrary numbers of type-I and type-II solitons. Section V concludes the paper.

II. DARK SOLITON SOLUTIONS TO CMKDV EQUATION

In this section, we first present the general dark soliton solutions of the cmKdV equation (2), which are expressed in terms of block determinants. When the determinant blocks are of specific orders, these general solutions reduce to two distinct types of dark solitons. We then analyze the properties of these two types of single dark solitons. They differ not only in their mathematical structures but also in their velocity-amplitude relations and valley profiles under detailed examination.

A. Explicit formulas for general dark soliton solutions of the cmKdV equation

We present the general dark soliton solutions to the cmKdV equation (2). A detailed derivation of these solutions is given in Appendix A.

Theorem 1. *The cmKdV equation (2) admits the following dark soliton solutions*

$$u = \frac{g}{f}, \quad (3)$$

where $f = \bar{\delta}_0, g = \bar{\delta}_1$, and

$$\bar{\delta}_n = \det \begin{pmatrix} \mathcal{M}_{i,j}^{[n,1,1]} & \mathcal{M}_{i,j}^{[n,1,2]} \\ \mathcal{M}_{i,j}^{[n,2,1]} & \mathcal{M}_{i,j}^{[n,2,2]} \end{pmatrix}, \quad (4)$$

with

$$\begin{aligned} \mathcal{M}_{i,j}^{[n,1,1]} &= \Gamma_1 + \left(\bar{m}_{i,j}^{(n)} \right)_{2N_1 \times 2N_1}, \quad \mathcal{M}_{i,j}^{[n,1,2]} = \left(\bar{m}_{i,2N_1+j}^{(n)} \right)_{2N_1 \times N_2}, \\ \mathcal{M}_{i,j}^{[n,2,1]} &= \left(\bar{m}_{2N_1+i,j}^{(n)} \right)_{N_2 \times 2N_1}, \quad \mathcal{M}_{i,j}^{[n,2,2]} = \Gamma_2 + \left(\bar{m}_{2N_1+i,2N_1+j}^{(n)} \right)_{N_2 \times N_2}, \\ \Gamma_1 &= \text{diag} (e^{-\zeta_1}, e^{-\zeta_2}, \dots, e^{-\zeta_{2N_1}}), \quad \Gamma_2 = \text{diag} (e^{-\zeta_{2N_1+1}}, e^{-\zeta_{2N_1+2}}, \dots, e^{-\zeta_{2N_1+N_2}}). \end{aligned} \quad (5)$$

Here,

$$\bar{m}_{i,j}^{(n)} = \frac{1}{p_i + p_j^*} \left(-\frac{p_i}{p_j^*} \right)^n, \quad \zeta_i = (p_i + p_i^*)x + [3(p_i + p_i^*) - (p_i^3 + p_i^{*3})]t + \zeta_{i,0}. \quad (6)$$

The parameters are subject to the following constraints

$$|p_i| = 1, \quad p_{N_1+s} = -p_s, \quad \zeta_{N_1+s,0} = -\zeta_{s,0} + i\pi \quad (7)$$

for $i = 1, 2, \dots, 2N_1 + N_2$ and $s = 1, 2, \dots, N_1$, with $p_i \in \mathbb{C}$ and $\zeta_{s,0} \in \mathbb{R}$.

Remark 1. In Eq. (7), the constraint $|p_i| = 1$ can be equivalently expressed as $p_i = e^{i\vartheta_i}$, where $\vartheta_i \in (-\pi, \pi)$. Under this form, the relation $p_{N_1+s} = -p_s$ becomes $e^{i\vartheta_{N_1+s}} = e^{i(\vartheta_s + \pi)}$. In the subsequent analysis of the properties and collisions of dark solitons, this representation will also be used to simplify related formulas.

Remark 2. Under the parameter restrictions in Eq. (7), the associated elements exhibit the following correlations:

$$\bar{m}_{N_1+s, N_1+\ell}^{(n)} = -\bar{m}_{s, \ell}^{(n)}, \quad \bar{m}_{N_1+s, \ell}^{(n)} = -\bar{m}_{s, N_1+\ell}^{(n)}, \quad e^{\zeta_{N_1+s}} = -e^{-\zeta_s}, \quad (8)$$

for $1 \leq s, \ell \leq N_1$. Specifically, when $N_2 = 0$, these correlations imply that the function $\bar{\delta}_n$, considered as a function of $\zeta_1, \zeta_2, \dots, \zeta_N$, satisfies the following symmetry:

$$\bar{\delta}_n(\zeta_1, \zeta_2, \dots, \zeta_{N_1}) = \bar{\delta}_n(-\zeta_1, -\zeta_2, \dots, -\zeta_{N_1}). \quad (9)$$

If we further set $\zeta_{s,0} = 0$ in the expression for ζ_i in Eq. (6), then $\bar{\delta}_n$ satisfies the following symmetry relation with respect to x and t :

$$\bar{\delta}_n(-x, -t) = \bar{\delta}_n(x, t). \quad (10)$$

Consequently, the dark soliton solutions given by Eq. (3) exhibit the symmetry

$$u(-x, -t) = u(x, t), \quad (11)$$

indicating that they are parity-time symmetric under the specific parameter conditions $N_2 = 0$ and $\zeta_{s,0} = 0$. In this case ($N_2 = 0$), the solutions of Eq. (3) correspond to a particular type of dark solitons, exhibiting double valleys, flat-bottom-shaped valleys, or single valleys, as will be discussed in detail later.

B. Dynamics of two types of single dark soliton solutions

As we briefly explained in Remark 2, when the orders N_1 and N_2 of the sub-blocks in the block determinants take different values, the block determinant solution (3) will correspond to different forms of solitons. It is necessary to study in detail the properties of the dark soliton solution (3) corresponding to the most specific values of N_1 and N_2 , namely $N_1 = 1, N_2 = 0$ and $N_1 = 0, N_2 = 1$, which represent two types of single dark solitons with different characteristics. When N_1 and N_2 in solution (3) take more general values, they correspond to the collisions of multiple dark soliton solutions of these two cases. To better distinguish these two types of solitons, we refer to the solutions (3) with $N_1 \neq 0, N_2 = 0$ as type-I dark solitons, and the solutions (3) with $N_1 = 0, N_2 \neq 0$ as type-II dark solitons. Naturally, the solution (3) with $N_1 N_2 \neq 0$ corresponds to a coexistence of type-I dark solitons and type-II dark solitons.

1. Dynamics of single type-I dark soliton

Setting $N_1 = 1, N_2 = 0$ in Eqs. (4)–(6), the associated functions f and g of solution (3) are expressed as

$$f = \begin{vmatrix} e^{-\zeta_1} + \bar{m}_{1,1}^{(0)} & \bar{m}_{1,2}^{(0)} \\ -\bar{m}_{1,2}^{(0)} & -e^{\zeta_1} - \bar{m}_{1,1}^{(0)} \end{vmatrix}, \quad g = \begin{vmatrix} e^{-\zeta_1} + \bar{m}_{1,1}^{(1)} & \bar{m}_{1,2}^{(1)} \\ -\bar{m}_{1,2}^{(1)} & -e^{\zeta_1} - \bar{m}_{1,1}^{(1)} \end{vmatrix}, \quad (12)$$

where

$$\bar{m}_{1,1}^{(n)} = \frac{1}{p_1 + p_1^*} \left(-\frac{p_1}{p_1^*} \right)^n, \quad \bar{m}_{1,2}^{(n)} = \frac{1}{p_1 - p_1^*} \left(\frac{p_1}{p_1^*} \right)^n, \quad \zeta_1 = (p_1 + p_1^*)x + [3(p_1 + p_1^*) - (p_1^3 + p_1^{*3})]t + \zeta_{1,0}, \quad (13)$$

and $|p_1| = 1$. From Eq. (3), a single soliton solution can be expressed in terms of hyperbolic functions as

$$u = \frac{\chi_0^{(1)} + \Theta_0^{(1)} \cosh(\zeta_1)}{\chi_0^{(0)} + \Theta_0^{(0)} \cosh(\zeta_1)}, \quad (14)$$

with $\chi_0^{(n)} = 1 - \frac{4}{(p_1^2 - p_1^{*2})^2} \left(\frac{p_1}{p_1^*} \right)^{2n}$ and $\Theta_0^{(n)} = \frac{2}{p_1 + p_1^*} \left(-\frac{p_1}{p_1^*} \right)^n$. As stated in Remark 2, this solution satisfies the symmetry $u(\zeta_1) = u(-\zeta_1)$. By setting $p_1 = e^{i\vartheta_1}$, Eq. (14) can be expressed in the equivalent form:

$$u = \frac{(\cot^2 2\vartheta_1 - \cos 2\vartheta_1 \sec \vartheta_1 \cosh \zeta_1) + 2i(\cot 2\vartheta_1 - \sin \vartheta_1 \cosh \zeta_1)}{1 + \csc^2(2\vartheta_1) + \sec \vartheta_1 \cosh \zeta_1}, \quad (15)$$

with $\zeta_1 = 2 \cos \vartheta_1 [x + (4 - 2 \cos 2\vartheta_1)t] + \zeta_{1,0}$, and $\vartheta_1 \in (-\pi, \pi), \zeta_{1,0} \in \mathbb{R}$. When one takes $\sec \vartheta_1 > 0$, i.e., $\vartheta_1 \in (-\frac{1}{2}\pi, \frac{1}{2}\pi)$, the denominator of this soliton solution remains strictly positive, so the soliton solution is smooth. The velocity of the soliton is given by

$$\nu = 2 \cos(2\vartheta_1) - 4. \quad (16)$$

In addition, $|u|$ approaches constant background amplitude 1 as $x \rightarrow \pm\infty$. As x varies from $-\infty$ to $+\infty$, the phase of u acquires no shift.

This dark soliton solution is characterized by the two parameters ϑ_1 (i.e., p_1) and $\zeta_{1,0}$. The parameter $\zeta_{1,0}$, which is embedded in ζ_1 , determines the position of the dark soliton. The parameter ϑ_1 not only influences the smoothness of the solution but also determines the waveform of the dark soliton, which in turn is governed by the sign of Δ_0 . Here, $\Delta_0 = \left(\partial_{\zeta_1 \zeta_1}^2 |u| \right) \Big|_{\zeta_1=0}$. Based on the sign of Δ_0 , the soliton can be classified into three types: a single-valley dark soliton when $\Delta_0 > 0$, a flat-bottom-shaped dark soliton when $\Delta_0 = 0$, and a double-valley dark soliton when $\Delta_0 < 0$. It is easy to verify that $(\partial_{\zeta_1} |u|) \Big|_{\zeta_1=0} = 0$, which indicates that if $|u(\zeta_1)|$ is regarded as a function of ζ_1 , then $\zeta_1 = 0$ is a critical point of $|u(\zeta_1)|$. When $\Delta_0 > 0$ (i.e., $\left. \frac{\partial^2 |u|}{\partial \zeta_1^2} \right|_{\zeta_1=0} > 0$), the point $\zeta_1 = 0$ is a local minimum of $|u(\zeta_1)|$. Thus, $|u|$ exhibits only one extremal line in the (x, t) plane, manifesting as a dark soliton with a single-valley profile. When $\Delta_0 = 0$, the point $\zeta_1 = 0$ is an inflection point of $|u(\zeta_1)|$, indicating that in the vicinity of $\zeta_1 = 0$ within the (x, t) plane, $|u|$ attains no extremum. Consequently, u in the (x, t) plane presents a dark soliton with flat-bottom-shaped profile. When $\Delta_0 < 0$ (i.e., $\left. \frac{\partial^2 |u|}{\partial \zeta_1^2} \right|_{\zeta_1=0} < 0$), the point $\zeta_1 = 0$ is a local maximum of $|u(\zeta_1)|$ in the vicinity of $\zeta_1 = 0$. In the detailed analysis below, this case will be shown to correspond to a dark soliton with a double-valley profile.

Next, we will specifically discuss the valley properties of these three types of solitons based on the sign of Δ_0 , where Δ_0 is explicitly formulated as

$$\Delta_0 = \frac{16 \sin^2 \vartheta_1 \cos^3 \vartheta_1 (8 \cos \vartheta_1 \sin^2 \vartheta_1 - 4 \cos^2 \vartheta_1 \sin^2 \vartheta_1 - 1)}{(4 \cos \vartheta_1 \sin^2 \vartheta_1 + 4 \cos^2 \vartheta_1 \sin^2 \vartheta_1 - 1)^2}. \quad (17)$$

The variation of the sign of Δ_0 with respect to ϑ_1 is shown in Fig. 1(a). This confirms that for suitable values of ϑ_1 , the conditions $\Delta_0 > 0$, $\Delta_0 = 0$, and $\Delta_0 < 0$ can all occur. When $\Delta_0 > 0$, $|u|$ has only one minimum at $\zeta_1 = 0$, and corresponds to a dark soliton with single-valley profile. Along the extremum $\zeta_1 = 0$, the intensity of this soliton is

$$\mathcal{I} = \sqrt{1 - \frac{16 \cos^3 \vartheta_1 \sin^2 \vartheta_1}{1 + 4 \cos \vartheta_1 \sin^2 \vartheta_1 (\cos \vartheta_1 + 1)}}. \quad (18)$$

When $\Delta_0 = 0$, namely, $\left(\partial_{\zeta_1 \zeta_1}^2 |u|\right) \Big|_{\zeta_1=0} = 0$, it also follows that $(\partial_{\zeta_1} |u|) \Big|_{\zeta_1=0} = 0$. This indicates that the center of the soliton at $\zeta_1 = 0$ is not an extremum of $|u|$. Therefore, $|u|$ exhibits a dark soliton with flat-bottom-shaped profile. The intensity of the flattop-shaped soliton is also given by Eq. (18). When $\Delta_0 < 0$, $|u|$ exhibits three extrema: one local maximum at $\zeta_1 = 0$ and two local minima at $\zeta_1 = \Lambda^\pm$, where

$$\Lambda^\pm = \ln \left[\frac{1}{\gamma_0} \left(\Lambda_0 \pm \sqrt{\Lambda_1} \right) \right], \quad (19)$$

with

$$\begin{aligned} \Lambda_0 &= 2 \sin^2(2\vartheta_1)(\cos 2\vartheta_1 - 2 \sin^4 \vartheta_1) + 1, & \gamma_0 &= 2 \sin \vartheta_1 \sin 2\vartheta_1 (\sin^2 2\vartheta_1 + 1), \\ \Lambda_1 &= \left[(\sin^2(2\vartheta_1) + 1)^2 - 16 \sin^2(2\vartheta_1) \cos^2 \vartheta_1 \right] \left[(\sin^2(2\vartheta_1) + 1)^2 - 4 \sin^2(2\vartheta_1) \cos^2 \vartheta_1 \right]. \end{aligned} \quad (20)$$

These extrema are identified by solving $\partial_{\zeta_1} |u| = 0$, and they satisfy the conditions $\partial_{\zeta_1 \zeta_1}^2 |u| \Big|_{\zeta_1=0} < 0$ and $\partial_{\zeta_1 \zeta_1}^2 |u| \Big|_{\zeta_1=\Lambda^\pm} > 0$. The extremum of $|u|$ at $\zeta_1 = 0$ is still expressed by Eq. (18). Along the other two extremum lines, the intensities of the dark soliton are equal and are given by

$$\bar{\mathcal{I}} = \frac{(2 \cos \vartheta_1^2 - 1)^2 |\sin \vartheta_1|}{\sqrt{16 \cos^8 \vartheta_1 - 48 \cos^6 \vartheta_1 + 40 \cos^4 \vartheta_1 - 8 \cos^2 \vartheta_1 + 1}}. \quad (21)$$

Since $\bar{\mathcal{I}} < \mathcal{I} < 1$, the valleys of the dark solitons, i.e., their minimum-intensity positions, are located at the two extremum lines $\zeta_1 = \Lambda^\pm$. Furthermore, since the two extrema are symmetric about $\zeta_1 = 0$ and have equal amplitudes, the soliton exhibits a symmetric double-valley profile.

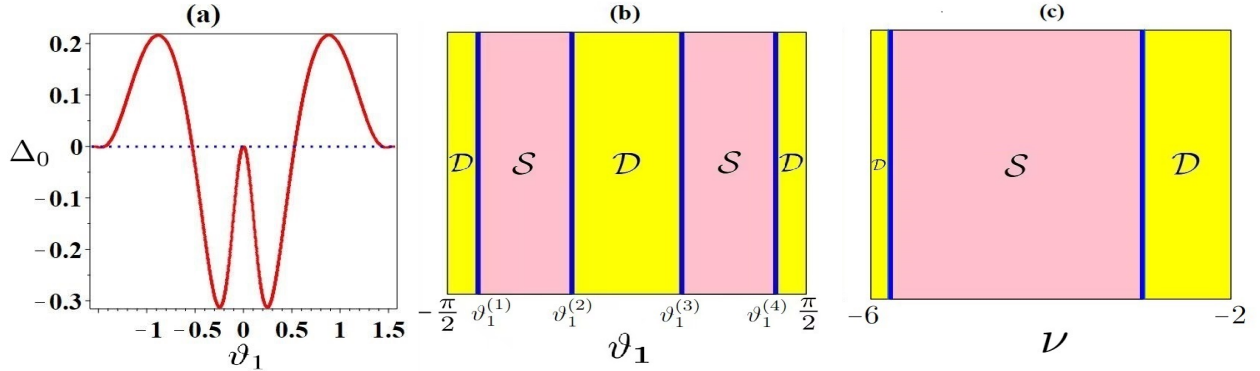


FIG. 1. (Color online) The valley profile alterations of the dark soliton solutions (15) as ϑ_1 varies: ‘ \mathcal{D} ’ represents double-valley (yellow region); ‘ \mathcal{S} ’ represents single-valley (pink region); and the blue solid line corresponds to the flat-bottom.

To better illustrate the correspondence between the soliton profiles and the range of values for ϑ_1 , we will revisit the relationship between the sign of Δ_0 and ϑ_1 . The condition $\Delta_0 = 0$ holds when ϑ_1 takes the values $\vartheta_1^{(1)}, \vartheta_1^{(2)}, \vartheta_1^{(3)}, \vartheta_1^{(4)}$, which correspond to the flat-bottom soliton. For $\vartheta_1 \in \left(-\frac{1}{2}\pi, \vartheta_1^{(1)}\right) \cup \left(\vartheta_1^{(2)}, \vartheta_1^{(3)}\right) \cup \left(\vartheta_1^{(4)}, \frac{1}{2}\pi\right)$, we have $\Delta_0 < 0$, leading to a double-valley-shaped dark soliton. Conversely, for $\vartheta_1 \in \left(\vartheta_1^{(1)}, \vartheta_1^{(2)}\right) \cup \left(\vartheta_1^{(3)}, \vartheta_1^{(4)}\right)$, the condition $\Delta_0 > 0$ holds, resulting in a single-valley-shaped dark soliton. Here $\vartheta_1^{(1,2,3,4)}$ are given as

$$\begin{aligned} \vartheta_1^{(1)} &= \arctan \left(-\frac{\sqrt{-2 + 2\sqrt{5} - 2\sqrt{5} + 2\sqrt{5}}}{1 - \sqrt{5} - 2\sqrt{5}} \right), & \vartheta_1^{(2)} &= \arctan \left(-\frac{\sqrt{-2 - 2\sqrt{5} - 2\sqrt{5} + 2\sqrt{5}}}{1 + \sqrt{5} - 2\sqrt{5}} \right), \\ \vartheta_1^{(3)} &= \arctan \left(\frac{\sqrt{-2 - 2\sqrt{5} - 2\sqrt{5} + 2\sqrt{5}}}{1 + \sqrt{5} - 2\sqrt{5}} \right), & \vartheta_1^{(4)} &= \arctan \left(\frac{\sqrt{-2 + 2\sqrt{5} - 2\sqrt{5} + 2\sqrt{5}}}{1 - \sqrt{5} - 2\sqrt{5}} \right). \end{aligned} \quad (22)$$

The variations in the valley profiles of the dark soliton solutions (15) as ϑ_1 changes are shown in Fig. 1(b). It is clear that the transition from a double-valley to a single-valley profile necessarily passes through an intermediate flat-bottom profile.

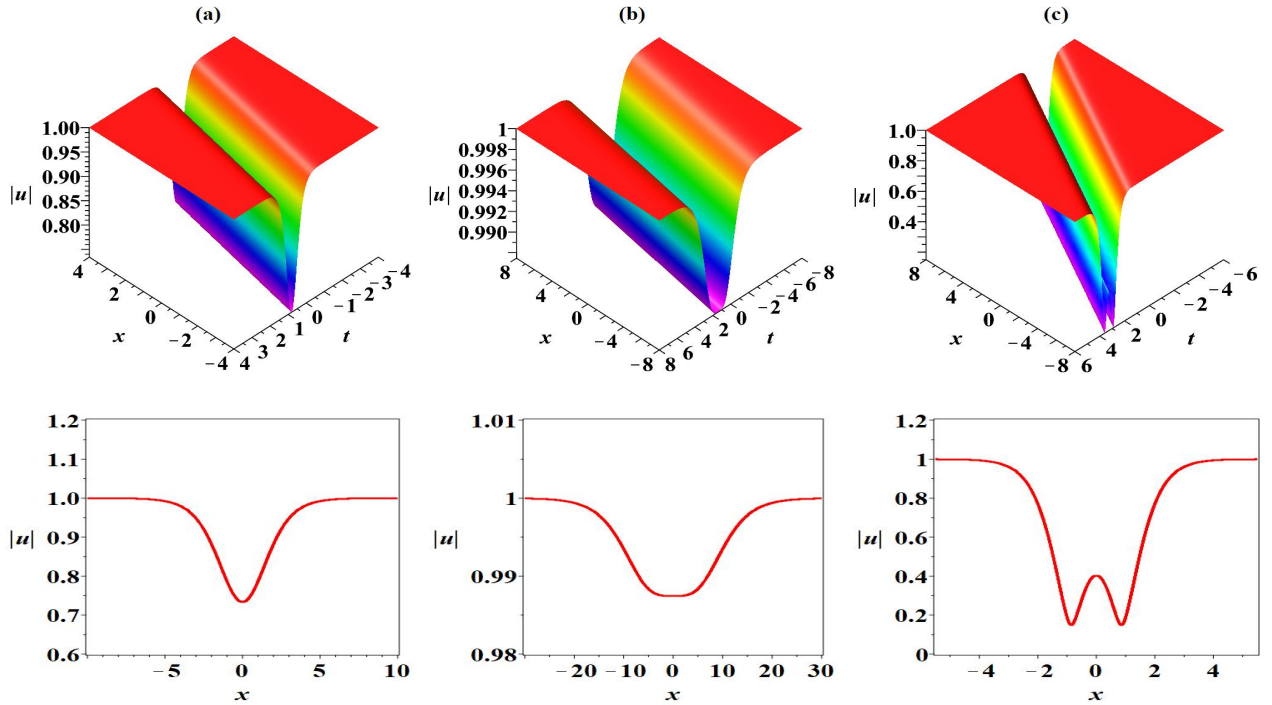


FIG. 2. (Color online) The dark soliton solutions (15) with three distinct valley profiles: (a) the single-valley-shaped profiles with parameters $\vartheta_1 = \frac{\pi}{3}$, $\bar{\zeta}_{1,0} = 0$; (b) the flat-bottom-shaped profile with parameters $\vartheta_1 = \arctan\left(\frac{\sqrt{-2+2\sqrt{5}}-2\sqrt{5}}{1-\sqrt{5-2\sqrt{5}}}\right)$, $\bar{\zeta}_{1,0} = 0$; (c) the double-valley-shaped profiles with parameters $\vartheta_1 = \frac{\pi}{9}$, $\bar{\zeta}_{1,0} = 0$. The bottom panels are intensity plots at $t = 0$.

The single dark soliton solution (15) with its three distinct valley profiles is illustrated in Fig. 2, corresponding to the conditions $\Delta_0 > 0$, $\Delta_0 = 0$, and $\Delta_0 < 0$, respectively.

Finally, we establish the relationship between the velocity ν and the valley profiles of the single type-I soliton. Since the relation between ϑ_1 and ν is given in Eq. (16), the dependence of the valley profiles on ϑ_1 in Fig. 1(b) can be equivalently expressed in terms of the velocity ν , as illustrated in Fig. 1(c).

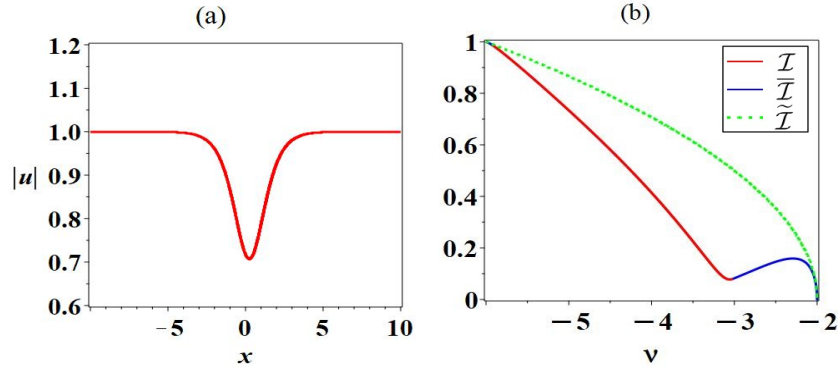


FIG. 3. (Color online) (a) The intensity plot of type-II dark soliton solutions (24) at $t = 0$ with parameters $\vartheta_1 = \frac{\pi}{3}$ and $\zeta_{1,0} = 0$. (b) The amplitude-velocity relations of the two types of single dark soliton solutions in Eqs. (15) and (24).

2. Dynamics of single type-II dark solitons

By setting $N_1 = 0$ and $N_2 = 1$ in Eqs. (4)–(6), the single type-II dark soliton solution can be derived as

$$u = \frac{e^{-\zeta_1} - \frac{1}{2}e^{2i\vartheta_1} \sec \vartheta_1}{e^{-\zeta_1} + \frac{1}{2} \sec \vartheta_1}. \quad (23)$$

To make the difference between this type-II soliton solution and the type-I dark soliton in Eq. (15) more evident at the level of mathematical expressions, it can be rewritten as

$$u = -\frac{1}{2} \left[e^{2i\vartheta_1} - 1 + (e^{2i\vartheta_1} + 1) \tanh \frac{\zeta_1 + \zeta_0}{2} \right], \quad (24)$$

with $\zeta_0 = -\ln(2 \cos \vartheta_1)$. As x varies from $-\infty$ to $+\infty$, the phase of u changes by $(\pi + 2\vartheta_1)$. The magnitude $|u|$ has a single extremum at $\zeta_1 + \zeta_0 = 0$, where it attains its minimum value,

$$\tilde{\mathcal{I}} = |\sin \vartheta_1|. \quad (25)$$

Hence, this dark soliton always has a single-valley profile. Its velocity coincides with that of the type-I dark soliton in Eq. (15), and is also given by Eq. (16). Therefore, the relationship between the amplitude and velocity of this single valley soliton can be expressed by the following function:

$$\nu = -4\tilde{\mathcal{I}}^2 - 2. \quad (26)$$

An example of this profile is displayed in Fig. 3(a).

Finally, we summarize the main differences between these two types of solitons:

- (i) The type-I dark solitons in Eq. (15) acquire no phase shift as x varies from $-\infty$ to $+\infty$, whereas the phase of the type-II dark soliton shifts by an amount of $(\pi + 2\vartheta_1)$ as x varies from $-\infty$ to $+\infty$;
- (ii) The type-I dark solitons exhibit three distinct valley profiles: double-valley, single-valley, and flat-bottom, while the type-II dark soliton only exhibits a single-valley profile;
- (iii) The two types of dark solitons obey different amplitude-velocity relations. To further visually emphasize the differences in velocity and amplitude between these two types of solitons, we present the evolution of amplitude with velocity in Fig. 3(b). Additionally, it can be directly inferred from the figure that the velocity is closely related to the valley profile of the type-I dark soliton. There are exactly two velocity intervals in which the type-I dark soliton exhibits a double-valley profile (corresponding to the velocity intervals of the blue line), while in a broader velocity interval, the type-I dark soliton displays a single-valley profile.

III. COLLISIONS BETWEEN TWO DARK SOLITON SOLUTIONS

The solution (3) represents two dark solitons when the condition $N_1 + N_2 = 2$ is satisfied in Eqs. (4)–(7). These two solitons can exhibit three different configurations depending on the values of N_1 and N_2 : (i) two type-I dark solitons for $N_1 = 2$ and $N_2 = 0$; (ii) two type-II dark solitons for $N_1 = 0$ and $N_2 = 2$; (iii) a mixture of one type-I dark soliton and one type-II dark soliton for $N_1 = 1$ and $N_2 = 1$. In what follows, we analytically examine the dynamics of these three kinds of two-soliton collisions.

For convenience, we denote the type-I soliton along the trajectory $\zeta_{k_1} \simeq \mathcal{O}(1)$ as \mathbf{S}_{k_1} , and the type-II soliton along the trajectory $\zeta_{2N_1+k_2} \simeq \mathcal{O}(1)$ as $\bar{\mathbf{S}}_{k_2}$, where $k_1 = 1, 2, \dots, N_1$ and $k_2 = 1, 2, \dots, N_2$. The asymptotic expressions of \mathbf{S}_{k_1} as $t \rightarrow \pm\infty$ are denoted by $u_{k_1}^\pm$, while those of $\bar{\mathbf{S}}_{k_2}$ are denoted by $\bar{u}_{k_2}^\pm$. Our asymptotic analysis will be performed under the following velocity ordering:

$$\nu_1 < \dots < \nu_{k_1} < \dots < \nu_{N_1} < \bar{\nu}_1 < \dots < \bar{\nu}_{k_2} < \dots < \bar{\nu}_{N_2} < 0, \quad (27)$$

where ν_{k_1} and $\bar{\nu}_{k_2}$, the velocities of \mathbf{S}_{k_1} and $\bar{\mathbf{S}}_{k_2}$, are defined by

$$\begin{aligned} \nu_{k_1} &= 2 \cos(2\vartheta_{k_1}) - 4, \\ \bar{\nu}_{k_2} &= 2 \cos(2\vartheta_{2N_1+k_2}) - 4. \end{aligned} \quad (28)$$

A. Collisions between two type-I dark solitons

By setting $N_1 = 2$ and $N_2 = 0$ in Eqs. (4)–(7), the solution (3) represents two type-I dark solitons, with associated functions f and g given by

$$f = \begin{vmatrix} e^{-\zeta_1} + \bar{m}_{1,1}^{(0)} & \bar{m}_{1,2}^{(0)} & \bar{m}_{1,3}^{(0)} & \bar{m}_{1,4}^{(0)} \\ \bar{m}_{2,1}^{(0)} & e^{-\zeta_2} + \bar{m}_{2,2}^{(0)} & \bar{m}_{2,3}^{(0)} & \bar{m}_{2,4}^{(0)} \\ -\bar{m}_{1,3}^{(0)} & -\bar{m}_{1,4}^{(0)} & -e^{\zeta_1} - \bar{m}_{1,1}^{(0)} & -\bar{m}_{1,2}^{(0)} \\ -\bar{m}_{2,3}^{(0)} & -\bar{m}_{2,4}^{(0)} & -\bar{m}_{2,1}^{(0)} & -e^{\zeta_2} - \bar{m}_{2,2}^{(0)} \end{vmatrix},$$

$$g = \begin{vmatrix} e^{-\zeta_1} + \bar{m}_{1,1}^{(1)} & \bar{m}_{1,2}^{(1)} & \bar{m}_{1,3}^{(1)} & \bar{m}_{1,4}^{(1)} \\ \bar{m}_{2,1}^{(1)} & e^{-\zeta_2} + \bar{m}_{2,2}^{(1)} & \bar{m}_{2,3}^{(1)} & \bar{m}_{2,4}^{(1)} \\ -\bar{m}_{1,3}^{(1)} & -\bar{m}_{1,4}^{(1)} & -e^{\zeta_1} - \bar{m}_{1,1}^{(1)} & -\bar{m}_{1,2}^{(1)} \\ -\bar{m}_{2,3}^{(1)} & -\bar{m}_{2,4}^{(1)} & -\bar{m}_{2,1}^{(1)} & -e^{\zeta_2} - \bar{m}_{2,2}^{(1)} \end{vmatrix}, \quad (29)$$

where $\bar{m}_{i,j}^{(n)}$ and ζ_i are defined in Eq. (6), subject to $|p_i| = 1$ with $p_3 = -p_1$ and $p_4 = -p_2$. The two type-I dark solitons are located along $\zeta_1 \simeq \mathcal{O}(1)$ and $\zeta_2 \simeq \mathcal{O}(1)$, with velocities $\nu_1 = 2 \cos(2\vartheta_1) - 4$ and $\nu_2 = 2 \cos(2\vartheta_2) - 4$. Here $|p_i| = 1$ is equivalently written as $p_i = e^{i\vartheta_i}$. We denote the solitons by \mathbf{S}_1 and \mathbf{S}_2 , with velocity ordering $\nu_1 < \nu_2 < 0$, to distinguish them in the subsequent asymptotic analysis. As before, we impose $\sec \vartheta_i > 0$ to ensure smoothness of the solution. Along the trajectories $\zeta_1 \simeq \mathcal{O}(1)$ and $\zeta_2 \simeq \mathcal{O}(1)$, as well as in the limits $t \rightarrow \pm\infty$, the asymptotic expressions for these two solitons are organized as follows:

(a) Before collision $t \rightarrow -\infty$

Soliton \mathbf{S}_1 ($\zeta_1 \simeq \mathcal{O}(1)$, $\zeta_2 \rightarrow +\infty$):

$$u_1^- \simeq \frac{\chi_1^{(1)} + \Theta_1^{(1)} \cosh(\zeta_1 + \Omega_1)}{\chi_1^{(0)} + \Theta_1^{(0)} \cosh(\zeta_1 + \Omega_1)}, \quad (30)$$

Soliton \mathbf{S}_2 ($\zeta_2 \simeq \mathcal{O}(1)$, $\zeta_1 \rightarrow -\infty$):

$$u_2^- \simeq \frac{\chi_2^{(1)} + \Theta_2^{(1)} \cosh(\zeta_2 + \Omega_2)}{\chi_2^{(0)} + \Theta_2^{(0)} \cosh(\zeta_2 + \Omega_2)}, \quad (31)$$

where

$$\begin{aligned} \chi_1^{(n)} &= \left(-\frac{p_2}{p_2^*} \right)^n \frac{1}{p_2 + p_2^*} \left[1 - \left(\frac{p_1}{p_1^*} \right)^{2n} \frac{4|p_1^2 - p_2^2|^2}{(p_1^2 - p_1^{*2})^2 |p_1^2 - p_2^{*2}|^2} \right], \\ \chi_2^{(n)} &= \left(-\frac{p_1}{p_1^*} \right)^n \frac{1}{p_1 + p_1^*} \left[1 - \left(\frac{p_2}{p_2^*} \right)^{2n} \frac{4|p_1^2 - p_2^2|^2}{(p_2^2 - p_2^{*2})^2 |p_1^2 - p_2^{*2}|^2} \right], \\ \Theta_1^{(n)} &= \frac{2}{(p_1 + p_1^*)(p_2 + p_2^*)} \left| \frac{p_1^2 - p_2^2}{p_1^2 - p_2^{*2}} \right| \left(\frac{p_1 p_2}{p_1^* p_2^*} \right)^n, \quad n = 0, 1, \\ \Omega_1 &= \ln \left| \frac{(p_1 - p_2)(p_1 - p_2^*)}{(p_1 + p_2)(p_1 + p_2^*)} \right|, \quad \Theta_2^{(n)} = \Theta_1^{(n)}, \quad \Omega_2 = -\Omega_1. \end{aligned} \quad (32)$$

(b) After collision $t \rightarrow +\infty$

Soliton \mathbf{S}_1 ($\zeta_1 \simeq \mathcal{O}(1)$, $\zeta_2 \rightarrow -\infty$):

$$u_1^+ \simeq \frac{\chi_1^{(1)} + \Theta_1^{(1)} \cosh(\zeta_1 - \Omega_1)}{\chi_1^{(0)} + \Theta_1^{(0)} \cosh(\zeta_1 - \Omega_1)}, \quad (33)$$

Soliton \mathbf{S}_2 ($\zeta_2 \simeq \mathcal{O}(1)$, $\zeta_1 \rightarrow +\infty$):

$$u_2^+ \simeq \frac{\chi_2^{(1)} + \Theta_2^{(1)} \cosh(\zeta_2 - \Omega_2)}{\chi_2^{(0)} + \Theta_2^{(0)} \cosh(\zeta_2 - \Omega_2)}. \quad (34)$$

The asymptotic analysis above directly implies that

$$u_1^+(\zeta_1) = u_1^-(\zeta_1 + \Delta\Phi_1), \quad u_2^+(\zeta_2) = u_2^-(\zeta_2 + \Delta\Phi_2), \quad (35)$$

where $\Delta\Phi_1, \Delta\Phi_2$ represent the phase shifts of solitons \mathbf{S}_1 and \mathbf{S}_2 during their collisions, respectively. They are given explicitly by

$$\Delta\Phi_1 = -\Delta\Phi_2 = -2\Omega_1. \quad (36)$$

This indicates two properties: (i) the collisions between the two type-I dark solitons do not alter their shapes, resulting in elastic or shape-preserving collisions. (ii) the total phase shifts of the two solitons sum to zero, i.e., $\Delta\Phi_1 + \Delta\Phi_2 = 0$. Fig. 4 illustrates an example of a shape-preserving collision between a type-I dark soliton with a double-valley profile and a type-I dark soliton with a flat-bottom-shaped profile, demonstrating that both solitons retain their shape after the collision.

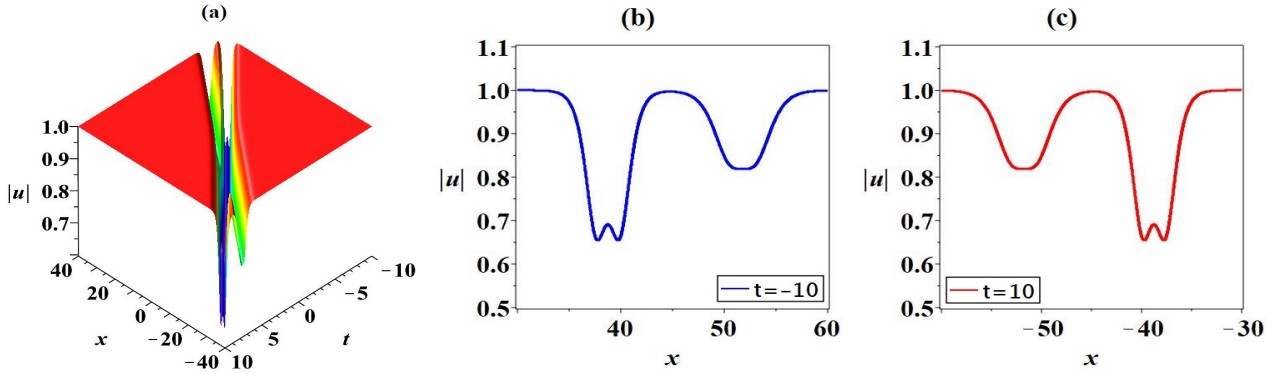


FIG. 4. (Color online) (a) The shape-preserving collisions of two type-I dark soliton solutions with $(p_1, p_2) = (e^{\frac{1}{3}i\pi}, e^{\frac{1}{4}i\pi})$ and $(\zeta_{1,0}, \zeta_{2,0}) = (0, 0)$. (b) and (c) are the intensity plots of the two type-I dark soliton solutions displayed in panel (a) at $t = -10$ and $t = 10$, respectively.

Although the collisions between these two solitons do not alter their shapes, one soliton can still influence the other. Specifically, altering the amplitude or velocity of one soliton will induce changes in the shape or amplitude of the other soliton, even if its velocity remains constant. Below, we will discuss the unique collision properties from two perspectives. Before that, we emphasize again that the velocity of soliton \mathbf{S}_{k_1} ($k_1 = 1, 2$) is determined solely by p_{k_1} ($p_{k_1} = e^{i\vartheta_{k_1}}$), with the magnitude of the velocity given by $\nu_{k_1} = 2\cos(\vartheta_{k_1}) - 4$. Changing the value of p_{k_1} (or ϑ_{k_1}) only affects the velocity of soliton \mathbf{S}_{k_1} without altering the velocity of the other soliton \mathbf{S}_{3-k_1} .

The first aspect concerns the relationship between the amplitudes of the two type-I solitons at their centers and their velocities. Since the amplitudes and shapes of the two type-I solitons remain unchanged before and after their collisions, we will only consider the amplitudes before the collisions and disregard those afterward. From the asymptotic expressions in Eqs. (30) and (31) for solitons \mathbf{S}_1 and \mathbf{S}_2 , it can be deduced that their amplitudes at their centers, where $\zeta_1 + \Omega_1^- = 0$ and $\zeta_2 + \Omega_2^- = 0$, are given by:

$$\begin{aligned} \mathcal{I}_1 &= |u_1^-| \Big|_{\zeta_1 = -\Omega_1^-} = \left| \frac{\chi_1^{(1)} + \Theta_1^{(1)}}{\chi_1^{(0)} + \Theta_1^{(0)}} \right|, \\ \mathcal{I}_2 &= |u_2^-| \Big|_{\zeta_2 = -\Omega_2^-} = \left| \frac{\chi_2^{(1)} + \Theta_2^{(1)}}{\chi_2^{(0)} + \Theta_2^{(0)}} \right|. \end{aligned} \quad (37)$$

Using the explicit expressions for $\chi_{k_1}^{(n)}$ and $\Theta_{k_1}^{(n)}$ in Eq. (32), we find that both \mathcal{I}_1 and \mathcal{I}_2 depend on p_1 and p_2 , which are related to the velocities of solitons \mathbf{S}_1 and \mathbf{S}_2 . Thus, the amplitudes of the two solitons are jointly determined by both velocities. To illustrate this correlation, we fix the velocity of one soliton, say ν_s ($s = 1$ or 2), and examine how \mathcal{I}_1 and \mathcal{I}_2 vary with the velocity ν_{3-s} of the other. For instance, if we take $p_1 = e^{\frac{1}{4}i\pi}$, then the velocity of soliton \mathbf{S}_1 is fixed at $\nu_1 = -4$. To satisfy the velocity constraint $\nu_1 < \nu_2 \leq 0$ required by our asymptotic analysis, we set the range of ϑ_2 ($p_2 = e^{i\vartheta_2}$) to $[\frac{\pi}{6}, \frac{\pi}{4})$, which corresponds to the velocity range of soliton \mathbf{S}_2 being $\nu_2 \in [-3, -4)$. Fig. 5(a) shows that while the amplitude \mathcal{I}_2 of soliton \mathbf{S}_2 varies with ν_2 , the amplitude \mathcal{I}_1 of soliton \mathbf{S}_1 also changes with ν_2 ,

even though ν_1 remains fixed. Similarly, by setting $p_2 = e^{\frac{1}{6}i\pi}$, we have $\nu_2 = -3$, fixing the velocity of soliton \mathbf{S}_2 . The numerical variations of \mathcal{I}_1 and \mathcal{I}_2 with respect to the velocity ν_1 of soliton \mathbf{S}_1 are shown in Fig. 5(b), further demonstrating this property.

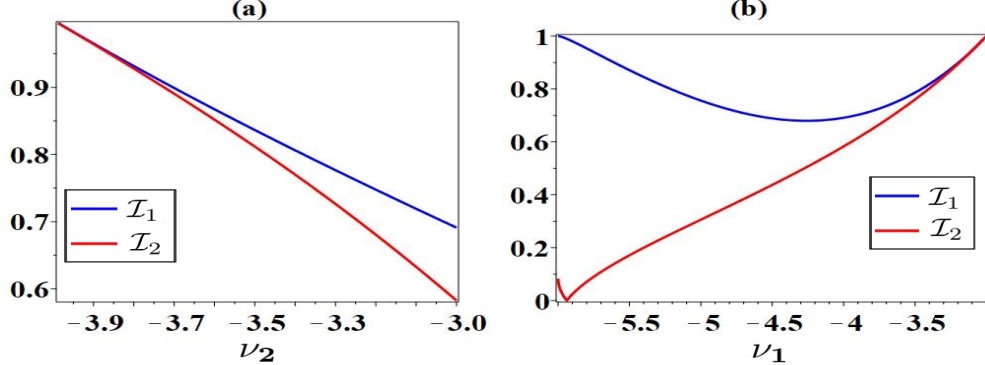


FIG. 5. (Color online) (a) The numerical variations of \mathcal{I}_1 and \mathcal{I}_2 with respect to the velocity ν_2 of soliton \mathbf{S}_2 , while the velocity of soliton \mathbf{S}_1 is fixed at $\nu_1 = -4$ (i.e., $p_1 = e^{\frac{1}{4}i\pi}$). (b) The numerical variations of \mathcal{I}_1 and \mathcal{I}_2 with respect to the velocity ν_1 of soliton \mathbf{S}_1 , while the velocity of soliton \mathbf{S}_2 is fixed at $\nu_2 = -3$ (i.e., $p_2 = e^{\frac{1}{6}i\pi}$).

The second aspect concerns the impact of the velocities of the two type-I solitons on their valley profiles(or soliton shapes). As in the single type-I dark soliton case, the valley profile of each soliton can be determined from the sign of Δ_{k_1} , where

$$\Delta_{k_1} = \left(\partial_{\zeta_{k_1} \zeta_{k_1}}^2 |u_{k_1}^-| \right) \Big|_{\zeta_{k_1} = -\Omega_{k_1}^-}, \quad k_1 = 1, 2. \quad (38)$$

The valley profiles of soliton \mathbf{S}_{k_1} can be classified into three categories according to the sign of Δ_{k_1} : double-valley when $\Delta_{k_1} < 0$, flat-bottom when $\Delta_{k_1} = 0$, and single-valley when $\Delta_{k_1} > 0$. It follows that Δ_{k_1} depends only on p_1 and p_2 , and hence on the velocities ν_1, ν_2 of the two type-I solitons. Due to the complexity of the specific algebraic expression of Δ_{k_1} in terms of ν_1 and ν_2 , the explicit form is not provided here. Specifically, the signs of Δ_1 and Δ_2 are determined simultaneously by the velocities ν_1 and ν_2 of the two solitons.

To illustrate this, we fix the velocity of soliton \mathbf{S}_2 at $\nu_2 = -4$ ($p_2 = e^{\frac{1}{4}i\pi}$). In this case, both Δ_1 and Δ_2 can be regarded as functions of ν_1 . The numerical evolution of Δ_1 and Δ_2 with respect to ν_1 is shown in Fig. 6(a). We observe that $\Delta_1, \Delta_2 > 0$ for $\nu_1 \in (-6, -5.5)$, indicating that both solitons are single-valley. By contrast, $\Delta_1, \Delta_2 < 0$ for $\nu_1 \in (-5, -4)$, so both solitons become double-valley. The detailed evolution of the shapes of solitons \mathbf{S}_1 and \mathbf{S}_2 as the velocity ν_1 of \mathbf{S}_1 varies is shown in Fig. 7. It clearly illustrates that while the velocity of soliton \mathbf{S}_2 remains fixed at $\nu_2 = -4$, the shapes of the solitons vary with changes in ν_1 . In Fig. 7(a), when the velocity of soliton \mathbf{S}_1 is $\nu_1 = 2 \cos(\frac{5}{6}\pi) - 4$, both solitons \mathbf{S}_1 and \mathbf{S}_2 are single-valley-shaped. However, when the velocity ν_1 changes to $\nu_1 = -5$ in Fig. 7(b), soliton \mathbf{S}_1 remains single-valley-shaped, while the shape of soliton \mathbf{S}_2 transforms to a double-valley shape. In particular, when the velocity ν_1 of soliton \mathbf{S}_1 changes to $\nu_1 = -4$ in Fig. 7(c), the shape of soliton \mathbf{S}_1 becomes flat-bottom-shaped, whereas the shape of soliton \mathbf{S}_2 remains double-valley-shaped. Finally, when the velocity of soliton \mathbf{S}_1 changes to $\nu_1 = 2 \cos(\frac{7}{12}\pi) - 4$ in Fig. 7(d), both solitons \mathbf{S}_1 and \mathbf{S}_2 are double-valley-shaped.

We further confirm that the valley profiles of solitons \mathbf{S}_1 and \mathbf{S}_2 vary with the velocity ν_2 of \mathbf{S}_2 , when \mathbf{S}_1 is fixed at $\nu_1 = -5$. This dependence is evident from the evolution of the sign of Δ_2 with respect to ν_2 , as shown in Fig. 6(b).

B. Collisions between two type-II dark solitons

Setting $N_1 = 0, N_2 = 1$ in Eqs.(4)–(7), the solution (3) corresponds to two type-II dark solitons, with associated functions f and g given by

$$\begin{aligned} f &= \begin{vmatrix} e^{-\zeta_1} + \bar{m}_{1,1}^{(0)} & \bar{m}_{1,2}^{(0)} \\ \bar{m}_{2,1}^{(0)} & e^{-\zeta_2} + \bar{m}_{2,2}^{(0)} \end{vmatrix}, \\ g &= \begin{vmatrix} e^{-\zeta_1} + \bar{m}_{1,1}^{(1)} & \bar{m}_{1,2}^{(1)} \\ \bar{m}_{2,1}^{(1)} & e^{-\zeta_2} + \bar{m}_{2,2}^{(1)} \end{vmatrix}, \end{aligned} \quad (39)$$

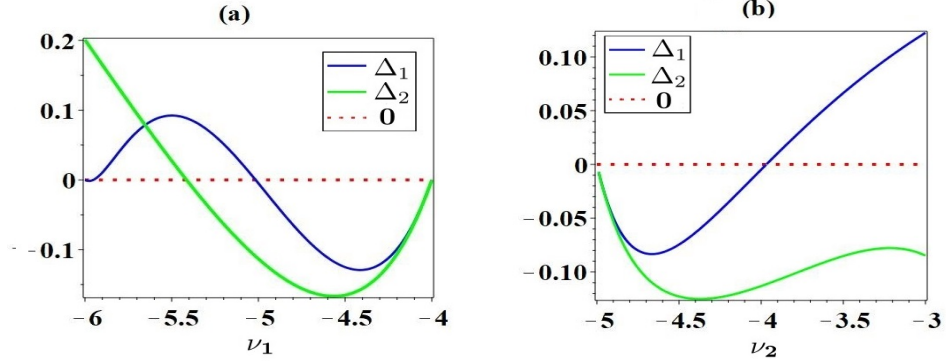


FIG. 6. (Color online) (a) The numerical variations of \mathcal{I}_1 and \mathcal{I}_2 with respect to the velocity ν_2 of soliton \mathbf{S}_2 , while the velocity of soliton \mathbf{S}_1 is fixed at $\nu_1 = -4$ (i.e., $p_1 = e^{\frac{1}{4}i\pi}$). (b) The numerical variations of \mathcal{I}_1 and \mathcal{I}_2 with respect to the velocity ν_1 of soliton \mathbf{S}_1 , while the velocity of soliton \mathbf{S}_2 is fixed at $\nu_2 = -3$ (i.e., $p_2 = e^{\frac{1}{6}i\pi}$).

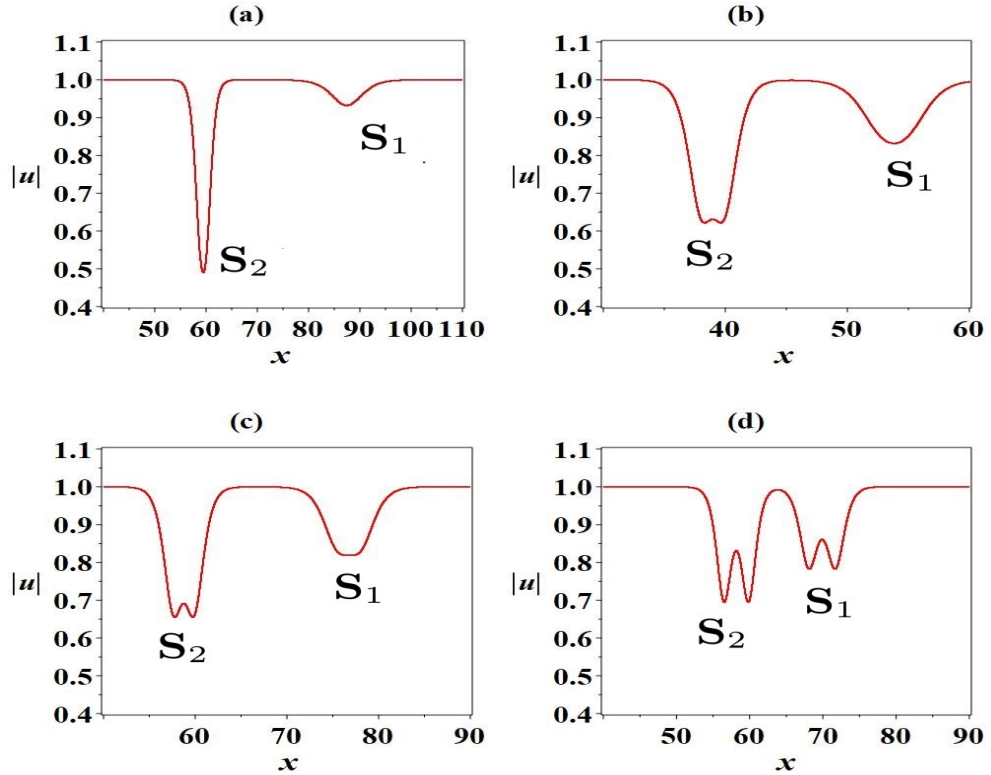


FIG. 7. (Color online) The shape alterations of two type-I dark solitons as the velocity ν_1 of \mathbf{S}_1 varies, with \mathbf{S}_2 fixed at $\nu_2 = -4$ ($p_2 = e^{\frac{1}{4}i\pi}$). The solutions (29) are plotted at $t = -15$ with $\zeta_{1,0} = \zeta_{2,0} = 0$: (a) two single-valley-shaped solitons with $\nu_1 = 2\cos(\frac{5}{6}\pi) - 4$ (i.e., $p_1 = e^{\frac{5}{12}i\pi}$); (b) a double-valley-shaped soliton coexisting with a single-valley-shaped soliton with $\nu_1 = 2\cos(\frac{17}{24}\pi) - 4$ (i.e., $p_1 = e^{\frac{17}{48}i\pi}$); (c) a double-valley-shaped soliton coexisting with a flat-bottom-shaped soliton with $\nu_1 = -5$ (i.e., $p_1 = e^{\frac{1}{3}i\pi}$); (d) two double-valley-shaped solitons with $\nu_1 = 2\cos(\frac{7}{12}\pi) - 4$ (i.e., $p_1 = e^{\frac{7}{24}i\pi}$).

where ζ_i and $m_{i,j}^{(n)}$ are explicitly given by Eq. (6). To reveal the collisions of the two type-II dark solitons, we also perform the asymptotic analysis for the two type-II dark solitons under the velocity constraint $\bar{\nu}_1 < \bar{\nu}_2 < 0$. After algebraic simplification, the asymptotic expression is concisely written in the following form:

$$\bar{u}_{k_2}^{\pm} \simeq -\frac{1}{2}\mu_{k_2}^{\pm} \left[e^{2i\vartheta_{k_2}} - 1 + (e^{2i\vartheta_{k_2}} + 1) \tanh \frac{\zeta_{k_2} + \bar{\Omega}_{k_2}^{\pm}}{2} \right], \quad k_2 = 1, 2, \quad (40)$$

where

$$\begin{aligned} \mu_1^- = \mu_2^+ &= 1, \quad \mu_1^+ = e^{i(2\vartheta_2 + \pi)}, \quad \mu_2^- = e^{i(2\vartheta_1 + \pi)}, \\ \bar{\Omega}_1^- &= \ln \left(\frac{1}{2 \cos \vartheta_1} \right), \quad \bar{\Omega}_1^+ = \bar{\Omega}_1^- + \Delta \bar{\Phi}, \quad \bar{\Omega}_2^- = \bar{\Omega}_2^+ + \Delta \bar{\Phi}, \\ \bar{\Omega}_2^+ &= \ln \left(\frac{1}{2 \cos \vartheta_2} \right), \quad \Delta \bar{\Phi} = 2 \ln \left| \frac{e^{i\vartheta_1} - e^{i\vartheta_2}}{e^{i\vartheta_1} + e^{-i\vartheta_2}} \right|. \end{aligned} \quad (41)$$

Here we take $p_1 = e^{i\vartheta_1}$ and $p_2 = e^{i\vartheta_2}$. The asymptotic expressions yield $|\bar{u}_1^+(\zeta_1)| = |\bar{u}_1^-(\zeta_1 + \Delta \bar{\Phi})|$ and $|\bar{u}_2^+(\zeta_2)| = |\bar{u}_2^-(\zeta_2 - \Delta \bar{\Phi})|$, showing that collisions between two type-II solitons are shape-preserving. One soliton acquires a phase shift $\Delta \bar{\Phi}$, the other $-\Delta \bar{\Phi}$, so the total phase shift vanishes. The amplitude of a soliton centered around $\zeta_k \simeq \mathcal{O}(1)$ is $\tilde{\mathcal{I}}_k = |\sin \vartheta_k|$, depends only on its own velocity and is independent of the other soliton. This characteristic is completely different from that of type-I solitons, where the amplitude of each soliton is dependent on the velocities of both solitons.

C. Collisions between a type-I dark soliton and a type-II dark soliton

Setting $N_1 = N_2 = 1$ in Eqs. (4)–(7), the solution (3) corresponds to a type-I dark soliton coexisting with a type-II dark soliton, and associated functions f and g given by

$$\begin{aligned} f &= \begin{vmatrix} e^{-\zeta_1} + \bar{m}_{1,1}^{(0)} & \bar{m}_{1,2}^{(0)} & \bar{m}_{1,3}^{(0)} \\ -\bar{m}_{1,2}^{(0)} & -e^{-\zeta_1} - \bar{m}_{1,1}^{(0)} & \bar{m}_{2,3}^{(0)} \\ \bar{m}_{1,3}^{(0)*} & \bar{m}_{2,3}^{(0)*} & e^{-\zeta_3} + \bar{m}_{3,3}^{(0)} \end{vmatrix}, \\ g &= \begin{vmatrix} e^{-\zeta_1} + \bar{m}_{1,1}^{(1)} & \bar{m}_{1,2}^{(1)} & \bar{m}_{1,3}^{(1)} \\ -\bar{m}_{1,2}^{(1)} & -e^{-\zeta_1} - \bar{m}_{1,1}^{(1)} & \bar{m}_{2,3}^{(1)} \\ \bar{m}_{1,3}^{(-1)*} & \bar{m}_{2,3}^{(-1)*} & e^{-\zeta_3} + \bar{m}_{3,3}^{(1)} \end{vmatrix}, \end{aligned} \quad (42)$$

where ζ_k and $\bar{m}_{i,j}^{(n)}$ are explicitly defined in Eq. (6). To reveal the collisions between the two mixed dark solitons, asymptotic analysis is performed for them under the velocity correlation $\nu_1 < \bar{\nu}_1 < 0$. Here $\nu_1 (= 2 \cos 2\vartheta_1 - 4)$ is the velocity of the type-I dark soliton and $\bar{\nu}_1 (= 2 \cos 2\vartheta_3 - 4)$ is the velocity of the type-II dark soliton. We denote the type-I dark soliton by \mathbf{S}_1 and the type-II dark soliton by $\bar{\mathbf{S}}_1$. After algebraic simplification, the asymptotic expression is concisely written in the following form:

(a) Before collision $t \rightarrow -\infty$

Soliton \mathbf{S}_1 ($\zeta_1 \simeq \mathcal{O}(1)$, $\zeta_3 \rightarrow +\infty$):

$$u_1^- \simeq \frac{\tilde{\chi}_1^{(1)-} + \tilde{\Theta}_1^{(1)-} \cosh(\zeta_1 + \tilde{\Omega}_1^-)}{\tilde{\chi}_1^{(0)-} + \tilde{\Theta}_1^{(0)-} \cosh(\zeta_1 + \tilde{\Omega}_1^-)}, \quad (43)$$

Soliton $\bar{\mathbf{S}}_1$ ($\zeta_3 \simeq \mathcal{O}(1)$, $\zeta_1 \rightarrow -\infty$):

$$\bar{u}_1^- \simeq -\frac{1}{2}\hat{\mu}_1^- \left[e^{2i\vartheta_3} - 1 + (e^{2i\vartheta_3} + 1) \tanh \frac{\zeta_3 + \hat{\Omega}_1^-}{2} \right], \quad (44)$$

where

$$\begin{aligned} \tilde{\chi}_1^{(n)-} &= -\left(-\frac{p_3}{p_3^*}\right)^n \frac{1}{p_3 + p_3^*} \left[1 - \left(\frac{p_1}{p_1^*}\right)^{2n} \frac{4|p_1^2 - p_3^2|^2}{(p_1^2 - p_1^{*2})^2 |p_1^2 - p_3^{*2}|^2} \right], \\ \tilde{\Theta}_1^{(n)-} &= -\frac{2}{(p_1 + p_1^*)(p_3 + p_3^*)} \left| \frac{p_1^2 - p_3^2}{p_1^2 - p_3^{*2}} \right| \left(\frac{p_1 p_3}{p_1^* p_3^*} \right)^n, \quad n = 0, 1, \\ \tilde{\Omega}_1^- &= \ln \left| \frac{(p_1 - p_3)(p_1 - p_3^*)}{(p_1 + p_3)(p_1 + p_3^*)} \right|, \quad \hat{\Omega}_1^- = \ln \left(\frac{1}{p_3 + p_3^*} \left| \frac{p_1 + p_3}{p_1 - p_3^*} \right|^2 \right), \quad \hat{\mu}_1^- = \hat{\mu}_1 = -\frac{p_1}{p_1^*}. \end{aligned} \quad (45)$$

(b) After collision $t \rightarrow +\infty$

Soliton \mathbf{S}_1 ($\zeta_1 \simeq \mathcal{O}(1), \zeta_3 \rightarrow -\infty$):

$$u_1^+ \simeq \frac{\tilde{\chi}_1^{(1)+} + \tilde{\Theta}_1^{(1)+} \cosh(\zeta_1)}{\tilde{\chi}_1^{(0)+} + \tilde{\Theta}_1^{(0)+} \cosh(\zeta_1)}, \quad (46)$$

Soliton $\bar{\mathbf{S}}_1$ ($\zeta_3 \simeq \mathcal{O}(1), \zeta_1 \rightarrow +\infty$):

$$\bar{u}_1^+ \simeq -\frac{1}{2} \hat{\mu}_1^+ \left[e^{2i\vartheta_3} - 1 + (e^{2i\vartheta_3} + 1) \tanh \frac{\zeta_3 + \hat{\Omega}_1^+}{2} \right], \quad (47)$$

where

$$\begin{aligned} \tilde{\chi}_1^{(n)+} &= 1 - \frac{4}{(p_1^2 - p_1^{*2})^2} \left(\frac{p_1}{p_1^*} \right)^{2n}, \quad \tilde{\Theta}_1^{(n)+} = \frac{2}{p_1 + p_1^*} \left(-\frac{p_1}{p_1^*} \right)^n, \quad n = 0, 1, \\ \hat{\Omega}_1^+ &= \ln \left(\frac{1}{p_3 + p_3^*} \left| \frac{p_1 - p_3}{p_1 + p_3^*} \right|^2 \right), \quad \hat{\mu}_1^+ = \hat{\mu}_1. \end{aligned} \quad (48)$$

Based on the above asymptotic expressions, we now analyze the collision dynamics of the two mixed-type solitons. First, the algebraic expressions of $\tilde{\chi}_1^{(n)\pm}$ and $\tilde{\Theta}_1^{(n)\pm}$ ($n = 0, 1$) imply that $|u_1^+(\zeta_1)| \neq |u_1^-(\zeta_1 + \Delta\tilde{\Phi}_1)|$, where $\Delta\tilde{\Phi}_1 = -\hat{\Omega}_1$ denotes the phase shift of the type-I dark soliton. This implies that the type-I dark soliton \mathbf{S}_1 undergoes a shape change after the collision. In contrast, since $|\bar{u}_1^+(\zeta_3)| = |\bar{u}_1^-(\zeta_3 + \Delta\hat{\Phi}_1)|$, where $\Delta\hat{\Phi}_1 = \hat{\Omega}_1^+ - \hat{\Omega}_1^-$ represents the phase shift experienced by the type-II dark soliton, this indicates that the type-II dark soliton maintains its shape after the collision. Therefore, since shape changes occur in the type-I dark soliton, the collision between these mixed-type solitons is classified as a shape-altering collision. A typical example of such a shape-altering collision is displayed in Fig. 8. In this example, the type-I soliton is double-valley-shaped at $t = -10$ but transforms into a single-valley shape at $t = 10$. In contrast, the type-II soliton $\bar{\mathbf{S}}_1$ maintains its shape throughout the process.

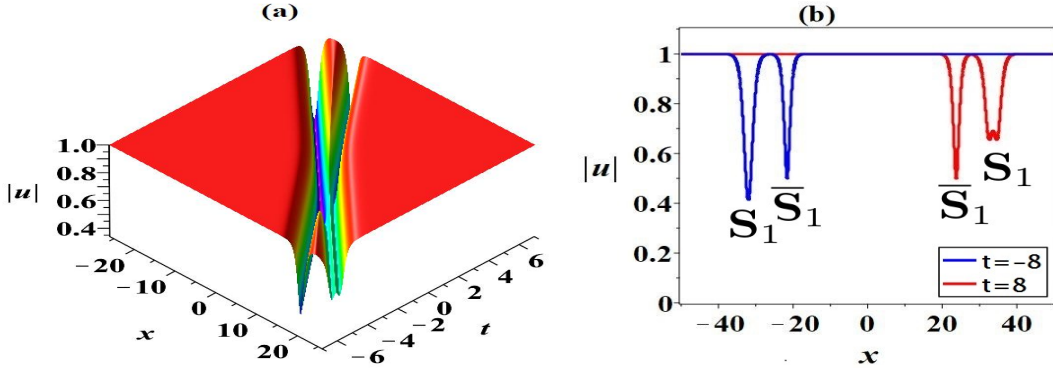


FIG. 8. (Color online) (a) The shape-altering collision between a type-I dark soliton and a type-II dark soliton with $(p_1, p_3) = (e^{\frac{1}{4}i\pi}, e^{\frac{1}{6}i\pi})$ and $(\zeta_{1,0}, \zeta_{3,0}) = (0, 0)$. (b) The intensity plot of the two solitons in panel (a) at $t = \pm 8$.

Second, we consider the asymptotic expression u_1^- of the type-I soliton \mathbf{S}_1 in Eq. (43) before the collision. The phase shift factor $\tilde{\Omega}_1^-$ and the shape-related factors $\tilde{\chi}_1^{(n)-}$ and $\tilde{\Theta}_1^{(n)-}$, are all expressed in terms of the parameters $p_1 (= e^{i\vartheta_1})$ and $p_3 (= e^{i\vartheta_3})$. Specifically, p_1 and p_3 correspond to the velocities of solitons \mathbf{S}_1 and $\bar{\mathbf{S}}_1$, respectively, where $\nu_1 = 2 \cos(2\vartheta_1) - 4$ and $\bar{\nu}_1 = 2 \cos(2\vartheta_3) - 4$. This implies that, prior to the collision, the shape of soliton \mathbf{S}_1 is influenced not only by its own velocity ν_1 , but also by the velocity $\bar{\nu}_1$ of the soliton $\bar{\mathbf{S}}_1$. In contrast, for the asymptotic expression u_1^+ of the type-I soliton \mathbf{S}_1 in Eq. (46) after the collision, only the phase shift factor $\hat{\Omega}_1^+$ remains dependent on the parameter p_3 , but the factors determining the soliton's shape, $\tilde{\chi}_1^{(n)+}$ and $\tilde{\Theta}_1^{(n)+}$, rely solely on p_1 and are independent of p_3 . Thus, after the collision, the shape of soliton \mathbf{S}_1 depends only on its own velocity ν_1 and is unaffected by the velocity $\bar{\nu}_1$ of soliton $\bar{\mathbf{S}}_1$. This observation can also be confirmed by examining the signs of factors $\tilde{\Delta}_1^\pm$, where $\tilde{\Delta}_1^- = (\partial_{\zeta_1 \zeta_1} |u_1^-|)|_{\zeta_1=-\tilde{\Omega}_1^-}$ and $\tilde{\Delta}_1^+ = (\partial_{\zeta_1 \zeta_1} |u_1^+|)|_{\zeta_1=0}$. The similar analysis for the shapes of the type-I

TABLE I. Summary of two-soliton collisions.

Collision type	Shape change	Phase shift	Center amplitude
Type-I + Type-I	Shape-preserving	$\Delta\Phi_1 = -\Delta\Phi_2$	$\mathcal{I}_{1,2}$ depend on (p_1, p_2) ; amplitudes jointly depend on (ν_1, ν_2)
Type-II + Type-II	Shape-preserving	$\Delta\bar{\Phi}_1 = -\Delta\bar{\Phi}_2$	$\tilde{\mathcal{I}}_k = \sin \vartheta_k $; each soliton depends only on its own ϑ_k
Type-I + Type-II	Shape-altering (Type-I changes; Type-II preserves)	Type-I: $\Delta\tilde{\Phi}_1 = -\tilde{\Omega}_1$, Type-II: $\Delta\hat{\Phi}_1 = \hat{\Omega}_1^+ - \hat{\Omega}_1^-$	Type-I: before collision depends on (p_1, p_3) , after only on p_1 ; Type-II depends solely on its own parameter

soliton based on the this factor has already been conducted in detail earlier, as shown in Fig. 2 and Fig. 6, along with the related discussions. Therefore, we do not repeat it here.

To provide a more intuitive illustration of this property, we present intensity plots in Fig. 9, showing a collision between a type-I dark soliton \mathbf{S}_1 with fixed velocity $\nu_1 = -5$ (i.e., $p_1 = e^{\frac{1}{3}i\pi}$) and a type-II dark soliton $\bar{\mathbf{S}}_1$ with varying velocity $\bar{\nu}_1$. The plots clearly demonstrate that, before the collision, the shape of soliton \mathbf{S}_1 evolves from a single-valley profile (panel (a)), to a flat-bottom profile (panel (b)), and finally to a double-valley profile (panel (c)) as $\bar{\nu}_1$ changes. After the collision, however, soliton \mathbf{S}_1 consistently retains a single-valley shape, showing no further alteration.

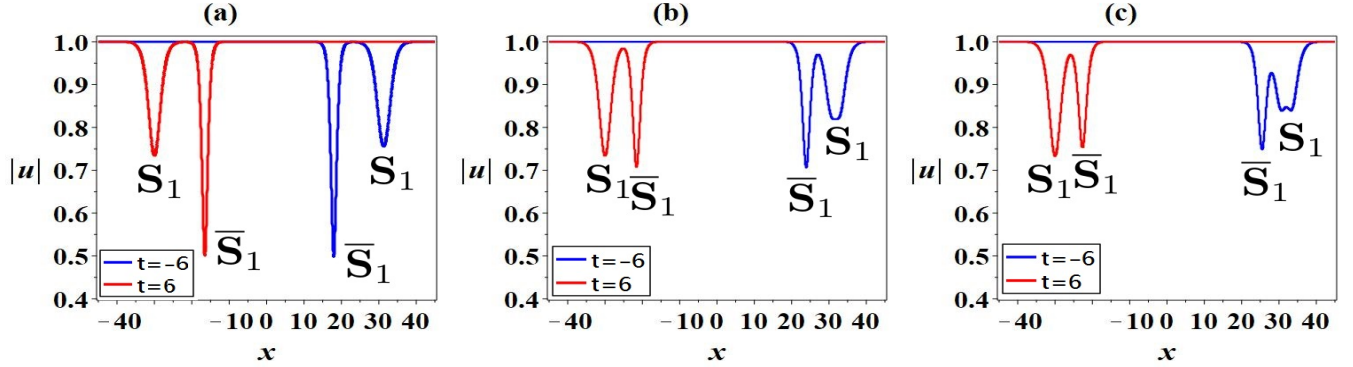


FIG. 9. (Color online) The shape-altering collisions of a type-I dark soliton with fixed velocity $\nu_1 = -5$ (i.e., $p_1 = e^{\frac{1}{3}i\pi}$) and a type-II dark soliton whose velocity $\bar{\nu}_1$ varies: (a) $\bar{\nu}_1 = -3$ (i.e., $p_3 = e^{\frac{1}{6}i\pi}$); (b) $\bar{\nu}_1 = -4$ (i.e., $p_3 = e^{\frac{1}{4}i\pi}$); (c) $\bar{\nu}_1 = 2 \cos(\frac{13}{24}\pi)$ (i.e., $p_3 = e^{\frac{13}{48}i\pi}$). The parameters $\zeta_{1,0}$ and $\zeta_{2,0}$ are set to 0.

Finally, we examine the shape changes of the type-I soliton \mathbf{S}_1 before and after the collision by analyzing its intensity profile along the soliton center. Before the collision, the center of \mathbf{S}_1 is located at $\zeta_1 + \tilde{\Omega}_1 = 0$, whereas after the collision it shifts to $\zeta_1 = 0$. Accordingly, the explicit expressions for the intensity of \mathbf{S}_1 along its center are

$$\begin{aligned} \mathcal{I}_1^- &= (|u_1^-|)|_{\zeta_1 = -\tilde{\Omega}_1^-} = \left| \frac{\tilde{\chi}_1^{(1)-} + \tilde{\Theta}_1^{(1)-}}{\tilde{\chi}_1^{(0)-} + \tilde{\Theta}_1^{(0)-}} \right|, \\ \mathcal{I}_1^+ &= (|u_1^+|)|_{\zeta_1 = 0} = \left| \frac{\tilde{\chi}_1^{(1)+} + \tilde{\Theta}_1^{(1)+}}{\tilde{\chi}_1^{(0)+} + \tilde{\Theta}_1^{(0)+}} \right|. \end{aligned} \quad (49)$$

From the explicit forms of $\tilde{\chi}_1^{(n)\pm}$ and $\tilde{\Theta}_1^{(n)\pm}$ ($n = 0, 1$) in Eqs. (45) and (48), we deduce that $\mathcal{I}_1^- = \mathcal{I}_1^-(p_1, p_3)$ and $\mathcal{I}_1^+ = \mathcal{I}_1^+(p_1)$. This indicates that \mathcal{I}_1^- is determined by the velocities ν_1 and $\bar{\nu}_1$ of both solitons \mathbf{S}_1 and $\bar{\mathbf{S}}_1$, while \mathcal{I}_1^+ is determined solely by the velocity ν_1 of soliton \mathbf{S}_1 . In other words, changing the velocity $\bar{\nu}_1$ of the type-II soliton $\bar{\mathbf{S}}_1$ affects amplitude \mathcal{I}_1^- of soliton \mathbf{S}_1 before collision, but the after collision amplitude \mathcal{I}_1^+ remains unchanged. This is different from the type-I and type-II soliton collision discussed earlier, in which changing the velocity of either soliton modifies its amplitude both before and after the collision, with the amplitudes remaining equal across the collision.

To provide a clear comparison of the three types of two-soliton interactions discussed above, we summarize their key dynamical characteristics in Table I.

IV. COLLISIONS BETWEEN N_1 TYPE-I AND N_2 TYPE-II DARK SOLITONS

In this section, we investigate collisions between arbitrary N_1 Type-I and N_2 Type-II dark solitons, with $\max\{N_1, N_2\} \geq 2$. This extends the two-soliton collisions discussed in Section III. Our analysis is divided into three cases according to the values of N_1 and N_2 :

- i) collisions among N_1 Type-I dark solitons, with $N_1 > 2$ and $N_2 = 0$;
- ii) collisions among N_2 Type-II dark solitons, with $N_1 = 0$ and $N_2 > 2$;
- iii) mixed collisions between N_1 Type-I and N_2 Type-II dark solitons, with $N_1 N_2 \neq 0$ and $\max\{N_1, N_2\} \geq 2$.

To investigate these soliton collisions in detail, we perform an asymptotic analysis as $t \rightarrow \pm\infty$ for both Type-I and Type-II dark solitons in the three cases outlined above.

A. Collisions among pure N_1 type-I dark solitons

This subsection considers collisions among pure N_1 Type-I dark solitons $\mathbf{S}_1, \mathbf{S}_2, \dots, \mathbf{S}_{N_1}$, described by the solutions of Eq. (3) with $N_1 > 2$ and $N_2 = 0$. To this end, we first present the asymptotic behavior of the functions $\bar{\delta}_n$ in Eq. (4) as $t \rightarrow \pm\infty$, which is summarized in the following lemma. The detailed derivations are given in Appendix B.

Lemma 1. *Assume that the velocities of the solitons $\mathbf{S}_1, \mathbf{S}_2, \dots, \mathbf{S}_{N_1}$ satisfy the ordering in Eq. (27) with $N_2 = 0$, i.e.,*

$$\nu_1 < \nu_2 < \dots < \nu_{k_1} < \dots < \nu_{N_1} < 0. \quad (50)$$

Along the trajectories $\zeta_{k_1} \simeq \mathcal{O}(1)$, the asymptotic form of $\bar{\delta}_n$ in Eq. (4) as $t \rightarrow \pm\infty$ is

$$\bar{\delta}_n^{(k_1)\pm} \simeq \rho_{k_1}^{\pm} \left(\chi_{k_1}^{(n)} + \Theta_{k_1}^{(n)} \cosh(\zeta_{k_1} \mp \Omega_{k_1}) \right) \quad (51)$$

where

$$\begin{aligned} \rho_{k_1}^- &= (-1)^{N_1-k_1+1} e^{\left(-\sum_{s=1}^{k_1-1} \zeta_s + \sum_{s=k_1+1}^{N_1} \zeta_s \right)} \mathcal{D}_{[k_1+1, N_1+k_1-1]}, \\ \rho_{k_1}^+ &= (-1)^{k_1} e^{\left(\sum_{s=1}^{k_1-1} \zeta_s - \sum_{s=k_1+1}^{N_1} \zeta_s \right)} \mathcal{D}_{[1, k_1-1] \cup [N_1+k_1+1, 2N_1]}, \\ \chi_{k_1}^{(n)} &= \left[\left(\prod_{s=1}^{k_1-1} \prod_{s=k_1+1}^{N_1} \right) \left(-\frac{p_s}{p_s^*} \right)^n \right] \left[1 - \left(-\frac{p_{k_1}}{p_{k_1}^*} \right)^{2n} \frac{4}{(p_{k_1}^2 - p_{k_1}^{*2})^2} \left(\prod_{s=1}^{k_1-1} \prod_{s=k_1+1}^{N_1} \right) \frac{|p_{k_1}^2 - p_s^2|^2}{|p_{k_1}^2 - p_s^{*2}|^2} \right], \\ \Theta_{k_1}^{(n)} &= \frac{2}{p_{k_1} + p_{k_1}^*} \left[\prod_{s=1}^{N_1} \left(-\frac{p_s}{p_s^*} \right)^n \right] \left[\left(\prod_{s=1}^{k_1-1} \prod_{s=k_1+1}^{N_1} \right) \frac{|p_{k_1}^2 - p_s^2|}{|p_{k_1}^2 - p_s^{*2}|} \right], \\ \Omega_{k_1} &= \ln \left[\left(\prod_{s=1}^{k_1-1} \frac{|p_s + p_{k_1}^*| |p_{k_1} + p_s|}{|p_{k_1} - p_s| |p_s - p_{k_1}^*|} \right) \left(\prod_{s=k_1+1}^{N_1} \frac{|p_{k_1} - p_s| |p_s - p_{k_1}^*|}{|p_s + p_{k_1}^*| |p_{k_1} + p_s|} \right) \right], \end{aligned} \quad (52)$$

for $k_1 = 1, 2, \dots, N_1$. Here, $\mathcal{D}_{[a,b]}$ denotes the Cauchy determinant with entries $\frac{1}{p_s + p_j^*}$, where the integer indices s and j range from a to b . Similarly, $\mathcal{D}_{[a,b] \cup [c,d]}$ represents the Cauchy determinant with entries $\frac{1}{p_s + p_j^*}$, where the indices s and j span the combined intervals $[a, b]$ and $[c, d]$. Since $\mathcal{D}_{[k_1+1, N_1+k_1-1]}$ and $\mathcal{D}_{[1, k_1-1] \cup [N_1+k_1+1, 2N_1]}$ will be eliminated in our final asymptotic expressions of type-I dark solitons, we do not provide their explicit algebraic expressions. The notation $\left(\prod_{s=a}^b \prod_{s=c}^d \right) f(s)$ represents two separate products over the same variable s : the first product is taken from $s = a$ to $s = b$, and the second from $s = c$ to $s = d$. This results in $\prod_{s=a}^b f(s) \cdot \prod_{s=c}^d f(s)$, which is the product of all $f(s)$ values in both ranges.

Using the explicit expression of $\bar{\delta}_n^{(k_1)\pm}$ in Eq. (51) of this lemma, the asymptotic expressions for each type-I dark soliton \mathbf{S}_{k_1} and the general solution (3) with $N_1 > 0, N_2 = 0$ can be yielded, as outlined by the following theorem.

Theorem 2. As $t \rightarrow \pm\infty$ and under the velocity correlation assumption in Eq. (50), the asymptotic expression for type-I dark soliton \mathbf{S}_{k_1} along $\zeta_{k_1} \simeq \mathcal{O}(1)$ in solution (3) with $N_1 > 0, N_2 = 0$ is

$$u_{k_1}^{\pm} \simeq \frac{\chi_{k_1}^{(1)} + \Theta_{k_1}^{(1)} \cosh(\zeta_{k_1} \mp \Omega_{k_1})}{\chi_{k_1}^{(0)} + \Theta_{k_1}^{(0)} \cosh(\zeta_{k_1} \mp \Omega_{k_1})}, \quad (53)$$

with $k_1 = 1, 2, \dots, N_1$. The asymptotics of solution (3) with $N_1 > 0, N_2 = 0$ is

$$|u^{\pm}| \simeq \sum_{k_1=1}^{N_1} |u_{k_1}^{\pm}| - (N_1 - 1). \quad (54)$$

We analyze the properties of the type-I dark solitons and their collisions based on the asymptotic expression (53). First, the center of type-I dark soliton \mathbf{S}_{k_1} shifts from

$$\zeta_{k_1} + \Omega_{k_1} = 0, \quad (55)$$

to

$$\zeta_{k_1} - \Omega_{k_1} = 0. \quad (56)$$

Thus the phase shift of this soliton undergoing during this collision is

$$\Delta\Phi_{k_1} = -2\Omega_{k_1}. \quad (57)$$

Specifically, since $\sum_{k_1=1}^{N_1} \Omega_{k_1} = 0$, it follows that

$$\sum_{k_1=1}^{N_1} \Delta\Phi_{k_1} = 0, \quad (58)$$

which implies that the total phase shifts of the N_1 solitons $\mathbf{S}_1, \mathbf{S}_2, \dots, \mathbf{S}_{N_1}$ also sum to zero.

Second, as the asymptotic expressions $u_{k_1}^-$ and $u_{k_1}^+$ admit the correlation:

$$u_{k_1}^+(\zeta_{k_1}) = u_{k_1}^-(\zeta_{k_1} + \Delta\Phi_{k_1}), \quad (59)$$

the collision between these N_1 pure type-I dark solitons are shape-preserving. Fig. 10 provides an example of such shape-preserving collision of three type-I dark solitons, illustrating that the type-I dark solitons $\mathbf{S}_1, \mathbf{S}_2, \mathbf{S}_3$ retain their double-valley profiles unaltered before and after collision. Here, we emphasize a comparison with the two type-I dark soliton collisions shown in Fig. 4. The parameters p_1, p_2 , and p_3 determine the velocities of the type-I solitons $\mathbf{S}_1, \mathbf{S}_2, \mathbf{S}_3$, respectively. In Fig. 10, the parameters p_1 and p_2 are taken the same values as those in Fig. 4, yet the velocities of solitons $\mathbf{S}_1, \mathbf{S}_2$ are identical in these two figures. However, the shapes of the solitons $\mathbf{S}_1, \mathbf{S}_2$ in Fig. 4 and Fig. 10 are completely different. This indicates that the participation of the type-I soliton \mathbf{S}_3 in the collision alters the shapes of the type-I dark soliton $\mathbf{S}_1, \mathbf{S}_2$. This phenomenon is related to the third property of pure type-I soliton collisions discussed below.

Our third aspect concerns the shapes of type-I dark solitons and the corresponding amplitudes of the solitons at their centers. Since type-I dark solitons only undergo shape-preserving collisions, we will focus solely on analyzing their shapes and amplitudes before their collisions, without considering the after collision outcomes. As we discussed earlier, the shape of the type-I dark soliton by \mathbf{S}_{k_1} determined by the sign of the factor Δ_{k_1} , where the factor Δ_{k_1} is given by:

$$\Delta_{k_1} = [\partial_{\zeta_{k_1} \zeta_{k_1}} (|u_{k_1}^-(\zeta_{k_1})|)]|_{\zeta_{k_1}=\Omega_{k_1}}, \quad k_1 = 1, 2, \dots, N_1. \quad (60)$$

The soliton \mathbf{S}_{k_1} is single-valley-shaped for $\Delta_{k_1} > 0$, flat-bottom-shaped for Δ_{k_1} and double-valley-shaped for $\Delta_{k_1} < 0$. One can easily verified that Δ_{k_1} is not only a function of p_k but also a function of p_1, p_2, \dots, p_N . Here, the parameter p_k determines the velocity of the soliton \mathbf{S}_{k_1} as $\nu_{k_1} = 2 \cos(2\vartheta_{k_1}) - 4$ if the parameter p_{k_1} is taken in its equivalent form $p_{k_1} = e^{i\vartheta_{k_1}}$. This implies that changing the velocity ν_{k_1} of a soliton \mathbf{S}_{k_1} will alter the shapes of all N_1 type-I solitons $\mathbf{S}_1, \mathbf{S}_2, \dots, \mathbf{S}_{N_1}$. In other words, these N_1 type-I dark solitons mutually influence the shapes of each other.

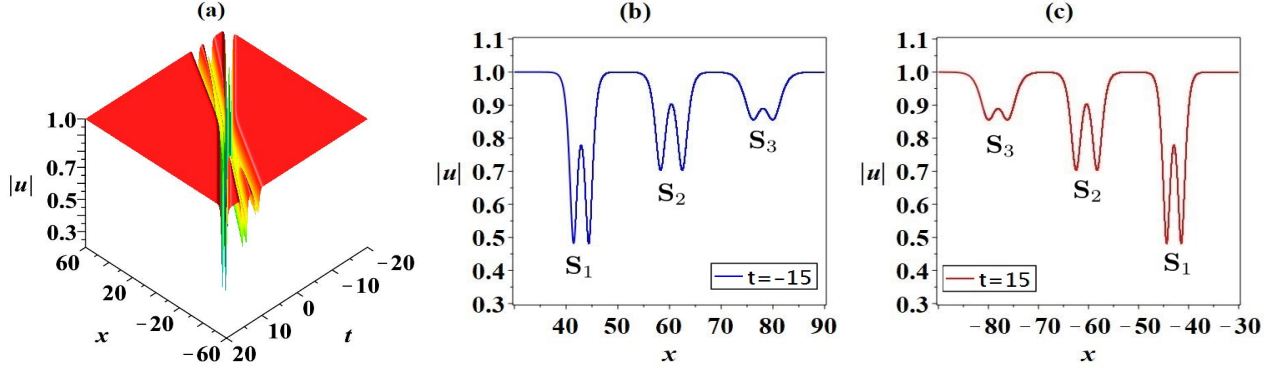


FIG. 10. (a) The shape-preserving collisions of three type-I dark soliton solutions with $(p_1, p_2, p_3) = (e^{\frac{1}{3}i\pi}, e^{\frac{1}{4}i\pi}, e^{\frac{1}{6}i\pi})$ and $(\zeta_{1,0}, \zeta_{2,0}, \zeta_{3,0}) = (0, 0, 0)$. (b) and (c) are the intensity plots of the three type-I dark soliton solutions displayed in panel (a) at $t = -15$ and $t = 15$, respectively.

This effect is also reflected in their amplitudes at their centers. The algebraic expression for the amplitude of the soliton \mathbf{S}_{k_1} at its center $\zeta_{k_1} - \Omega_{k_1} = 0$ is given by:

$$\mathcal{I}_{k_1} = |u_{k_1}^-| \Big|_{\zeta_{k_1} = \Omega_{k_1}} = \left| \frac{\chi_{k_1}^{(1)} + \Theta_{k_1}^{(1)}}{\chi_{k_1}^{(0)} + \Theta_{k_1}^{(0)}} \right|, \quad k_1 = 1, 2, \dots, N_1. \quad (61)$$

The value of \mathcal{I}_{k_1} is also determined by the parameters p_1, p_2, \dots, p_{N_1} collectively. This means that changing the amplitude of one type soliton will result in the amplitudes of all other type-I solitons being affected as well. This can be regarded as a generalization of the pure two dark solitons shown in Fig. 7. By changing the parameter equivalent to the velocity of one type-I soliton, the shapes and amplitudes of all type-I dark solitons will change.

B. Collisions among pure N_2 type-II dark solitons

This subsection focuses on the collisions among pure N_2 type-II dark solitons, described by the solutions (3) with $N_1 = 0$ and $N_2 > 2$. For this purpose, we first present the asymptotics of the functions $\bar{\delta}_n$ in Eq. (4) as $t \rightarrow \pm\infty$, summarized in the following lemma. The detailed derivations are given in Appendix B.

Lemma 2. *Assume that the velocities of the solitons $\bar{\mathbf{S}}_1, \bar{\mathbf{S}}_2, \dots, \bar{\mathbf{S}}_{N_2}$ satisfy the correlation in Eq. (27) with $N_1 = 0$, i.e.,*

$$\bar{v}_1 < \bar{v}_2 < \dots < \bar{v}_{k_2} < \dots < \bar{v}_{N_2} < 0, \quad (62)$$

then, along the soliton trajectories $\zeta_{k_2} \simeq \mathcal{O}(1)$ for $k_2 = 1, 2, \dots, N_2$, the asymptotic expression of the function $\bar{\delta}_n$ in Eq. (4) as $t \rightarrow \pm\infty$ is given by

$$\bar{\delta}_n^{(k_2)\pm} \simeq \bar{\rho}_{k_2}^{\pm} e^{-\zeta_{k_2}} (\mu_{k_2}^{\pm})^n \left[1 + (y_{k_2})^n e^{\zeta_{k_2} + \bar{\Omega}_{k_2}^{\pm}} \right], \quad (63)$$

where

$$\begin{aligned}
\bar{p}_{k_2}^- &= e^{\left(-\sum_{s=1}^{k_2-1} \zeta_s\right)} \left[\frac{\prod_{k_2+1 \leq s < j \leq N_2} (p_j - p_s) (p_j^* - p_s^*)}{\prod_{s,j=k_2+1}^{N_2} (p_s + p_j^*)} \right], \\
\bar{p}_{k_2}^+ &= e^{\left(-\sum_{s=k_2+1}^{N_2} \zeta_s\right)} \left[\frac{\prod_{1 \leq s < j \leq k_2-1} (p_j - p_s) (p_j^* - p_s^*)}{\prod_{s,j=1}^{k_2-1} (p_s + p_j^*)} \right], \\
\mu_{k_2}^- &= \prod_{s=k_2+1}^{N_2} \left(-\frac{p_s}{p_s^*} \right), \quad \mu_{k_2}^+ = \prod_{s=1}^{k_2-1} \left(-\frac{p_s}{p_s^*} \right), \quad y_{k_2} = -\frac{p_{k_2}}{p_{k_2}^*}, \\
\bar{\Omega}_{k_2}^- &= \ln \left[\frac{1}{p_{k_2} + p_{k_2}^*} \prod_{s=k_2+1}^{N_2} \frac{|p_s - p_{k_2}|^2}{|p_{k_2} + p_s^*|^2} \right], \quad \bar{\Omega}_{k_2}^+ = \ln \left[\frac{1}{p_{k_2} + p_{k_2}^*} \prod_{s=1}^{k_2-1} \frac{|p_s - p_{k_2}|^2}{|p_{k_2} + p_s^*|^2} \right].
\end{aligned} \tag{64}$$

for $k_2 = 1, 2, \dots, N_2$.

Using the explicit expression of $\bar{\delta}_n^{(k_2)\pm}$ in Eq. (63) of this lemma, the asymptotic expressions for each type-II dark soliton $\bar{\mathbf{S}}_{k_2}$ and the general solution (3) with $N_1 = 0$ and $N_2 > 0$ can be derived, as outlined in the following theorem.

Theorem 3. *As $t \rightarrow \pm\infty$ and under the velocity correlation assumption in Eq. (62), the asymptotic expression for type-II dark soliton $\bar{\mathbf{S}}_{k_2}$ in solution (3) with $N_1 = 0, N_2 > 0$ is*

$$\bar{u}_{k_2}^\pm \simeq \frac{1}{2} \mu_{k_2}^\pm \left[(1 + y_{k_2}) + (y_{k_2} - 1) \tanh\left(\frac{\zeta_{k_2} + \bar{\Omega}_{k_2}^\pm}{2}\right) \right] \tag{65}$$

with $k_2 = 1, 2, \dots, N_2$. The asymptotics of solution (3) with $N_1 = 0, N_2 > 0$ is

$$|u^\pm| \simeq \sum_{k_2=1}^{N_2} |\bar{u}_{k_2}^\pm| - (N_2 - 1). \tag{66}$$

We briefly summarize the collision properties of N_2 type-II dark solitons, as indicated by the asymptotic expressions (65) and (66). For the type-II dark soliton $\bar{\mathbf{S}}_{k_2}$, its center shifts from

$$\zeta_{k_2} + \bar{\Omega}_{k_2}^- = 0, \tag{67}$$

to

$$\zeta_{k_2} + \bar{\Omega}_{k_2}^+ = 0, \tag{68}$$

for $k_2 = 1, 2, \dots, N_2$. Thus, the phase shift of this soliton during the collision is

$$\Delta \bar{\Phi}_{k_2} = \bar{\Omega}_{k_2}^+ - \bar{\Omega}_{k_2}^-. \tag{69}$$

Specifically,

$$\sum_{k_2=1}^N \Delta \bar{\Phi}_{k_2} = 0, \tag{70}$$

indicating that the total phase shifts of all the N_2 solitons $\bar{\mathbf{S}}_1, \bar{\mathbf{S}}_2, \dots, \bar{\mathbf{S}}_{N_2}$ also sum to zero.

Since the modulus of the factors $\mu_{k_2}^\pm$ in the asymptotic expression $u_{k_2}^\pm$ of Eq. (65) is always unity, i.e., $|\mu_{k_2}^\pm| = 1$, the relationship between $|\bar{u}_{k_2}^-|$ and $|\bar{u}_{k_2}^+|$ can be expressed in the following form of phase-shift transformation:

$$|\bar{u}_{k_2}^+(\zeta_{k_2})| = |\bar{u}_{k_2}^-(\zeta_{k_2} + \Delta \bar{\Phi}_{k_2})|. \tag{71}$$

Thus, all N_2 type-II dark solitons generally maintain their shape and integrity, even after colliding with one another. Therefore, the collisions of pure N_2 type-II dark solitons are also shape-preserving.

Finally, the intensity of the type-II dark soliton $\bar{\mathbf{S}}_{k_2}$ at its center is

$$\tilde{\mathcal{I}}_{k_2} = |\sin \vartheta_{k_2}|, \quad (72)$$

where p_{k_2} is taken in the equivalent form $p_{k_2} = e^{i\vartheta_{k_2}}$. Accordingly, the velocity–amplitude correlation is expressed as

$$\bar{\nu}_{k_2} = -4\tilde{\mathcal{I}}_{k_2}^2 - 2. \quad (73)$$

This relation is consistent with that of a single type-II dark soliton given in Eq. (26), which confirms that the presence of other solitons does not affect the amplitude of $\bar{\mathbf{S}}_{k_2}$. In summary, collisions among pure N_2 type-II dark solitons are shape-preserving: the solitons undergo only phase shifts, while their individual profiles and amplitudes remain unchanged.

C. Collisions between mixed N_1 type-I and N_2 type-II dark solitons

This subsection considers the collisions between mixed type solitons consisting of N_1 type-I dark solitons and N_2 type-II dark solitons, depicted by the solutions (3) with $N_1 N_2 \neq 0$ and $\max\{N_1, N_2\} \geq 2$. For this purpose, we first derive the asymptotics of the functions $\bar{\delta}_n$ in Eq. (4) along the soliton trajectories as $t \rightarrow \pm\infty$, summarized in the following lemma.

Lemma 3. *Under the velocity conditions described in Eq. (27), the asymptotics of the function $\bar{\delta}_n$ along the trajectories of N_1 type-I dark solitons and N_2 type-II dark solitons are characterized as follows.*

- Along $\zeta_{k_1} \simeq \mathcal{O}(1)$, i.e., the trajectory of type-I dark soliton \mathbf{S}_{k_1} , the asymptotic expression of function $\bar{\delta}_n$ as $t \rightarrow \pm\infty$ is given by:

$$\bar{\delta}_n^{(k_1)\pm} \simeq \tilde{\rho}_{k_1}^{\pm} \left(\tilde{\chi}_{k_1}^{(n)\pm} + \tilde{\Theta}_{k_1}^{(n)\pm} \cosh(\zeta_{k_1} \mp \tilde{\Omega}_{k_1}^{\pm}) \right), \quad (74)$$

where

$$\begin{aligned} \tilde{\rho}_{k_1}^- &= (-1)^{N_1-k_1+1} e^{-\left(\sum_{s=1}^{k_1-1} \zeta_s\right) + \left(\sum_{s=k_1+1}^{N_1} \zeta_s\right)} \times \mathcal{D}_{[k_1+1, N_1+k_1-1] \cup [2N_1+1, 2N_1+N_2]}, \\ \tilde{\rho}_{k_1}^+ &= (-1)^{k_1} e^{\left(\sum_{s=1}^{k_1-1} \zeta_s\right) - \left(\sum_{s=k_1+1}^{N_1} \zeta_s\right) - \left(\sum_{s=2N_1+1}^{2N_1+N_2} \zeta_s\right)} \times \mathcal{D}_{[1, k_1-1] \cup [N_1+k_1+1, 2N_1]}, \\ \tilde{\chi}_{k_1}^{(n)-} &= \left[\left(\prod_{s=1}^{k_1-1} \prod_{s=k_1+1}^{N_1} \prod_{s=2N_1+1}^{2N_1+N_2} \right) \left(-\frac{p_s}{p_s^*} \right)^n \right] \\ &\quad \times \left[1 - \frac{4}{(p_{k_1}^2 - p_{k_1}^{*2})^2} \left(-\frac{p_{k_1}}{p_{k_1}^*} \right)^{2n} \left(\prod_{s=1}^{k_1-1} \prod_{s=k_1+1}^{N_1} \prod_{s=2N_1+1}^{2N_1+N_2} \right) \frac{|p_{k_1}^2 - p_s^2|^2}{|p_{k_1}^2 - p_s^{*2}|^2} \right], \\ \tilde{\Theta}_{k_1}^{(n)-} &= \frac{2}{p_{k_1} + p_{k_1}^*} \left[\left(\prod_{s=1}^{N_1} \prod_{s=2N_1+1}^{2N_1+N_2} \right) \left(-\frac{p_s}{p_s^*} \right)^n \right] \left[\left(\prod_{s=1}^{k_1-1} \prod_{s=k_1+1}^{N_1} \prod_{s=2N_1+1}^{2N_1+N_2} \right) \frac{|p_{k_1}^2 - p_s^2|}{|p_{k_1}^2 - p_s^{*2}|} \right], \\ \tilde{\Omega}_{k_1}^- &= \ln \left[\left(\prod_{s=1}^{k_1-1} \frac{|p_s + p_{k_1}^*| |p_{k_1} + p_s|}{|p_{k_1} - p_s| |p_s - p_{k_1}^*|} \right) \left(\prod_{s=k_1+1}^{N_1} \prod_{s=2N_1+1}^{2N_1+N_2} \right) \frac{|p_{k_1} - p_s| |p_s - p_{k_1}^*|}{|p_s + p_{k_1}^*| |p_{k_1} + p_s|} \right], \end{aligned} \quad (75)$$

and $\tilde{\chi}_{k_1}^{(n)+} = \chi_{k_1}^{(n)}$, $\tilde{\Theta}_{k_1}^{(n)+} = \Theta_{k_1}^{(n)}$, $\tilde{\Omega}_{k_1}^+ = -\Omega_{k_1}$, with $\chi_{k_1}^{(n)}$, $\Theta_{k_1}^{(n)}$, and Ω_{k_1} being defined by Eq. (52).

- Along $\zeta_{2N_1+k_2} \simeq \mathcal{O}(1)$, i.e., the trajectory of type-II dark soliton $\bar{\mathbf{S}}_{k_2}$, the asymptotic expression of function $\bar{\delta}_n$ as $t \rightarrow \pm\infty$ is given by:

$$\bar{\delta}_n^{(2N_1+k_2)\pm} \simeq \tilde{\rho}_{k_2}^{\pm} e^{-\zeta_{2N_1+k_2}} \left(\tilde{\mu}_{k_2}^{\pm} \right)^n \left[1 + \tilde{y}_{k_2}^n e^{\zeta_{2N_1+k_2} + \tilde{\Omega}_{k_2}^{\pm}} \right] \quad (76)$$

where

$$\begin{aligned}
\widehat{\rho}_{k_2}^- &= e^{-(\sum_{s=1}^{N_1} \zeta_s + \sum_{s=2N_1+1}^{2N_1+k_2-1} \zeta_s)} \mathcal{D}_{[N_1+1, 2N_1] \cup [2N_1+k_2+1, 2N_1+N_2]}, \\
\widehat{\rho}_{k_2}^+ &= (-1)^{N_1} e^{\sum_{s=1}^{N_1} \zeta_s - \sum_{s=2N_1+k_2+1}^{2N_1+N_2} \zeta_s} \mathcal{D}_{[1, N_1] \cup [2N_1+1, 2N_1+k_2-1]}, \quad \widehat{y}_{k_2} = -\frac{p_{2N_1+k_2}}{p_{2N_1+k_2}^*}, \\
\widehat{\mu}_{k_2}^- &= \left(\prod_{s=1}^{N_1} \prod_{s=2N_1+k_2+1}^{2N_1+N_2} \right) \left(-\frac{p_s}{p_s^*} \right), \quad \widehat{\mu}_{k_2}^+ = \left(\prod_{s=1}^{N_1} \prod_{s=2N_1+1}^{2N_1+k_2-1} \right) \left(-\frac{p_s}{p_s^*} \right), \\
\widehat{\Omega}_{k_2}^- &= \ln \left(\frac{1}{p_{2N_1+k_2} + p_{2N_1+k_2}^*} \prod_{s=1}^{N_1} \frac{|p_s + p_{2N_1+k_2}|^2}{|p_{2N_1+k_2} - p_s^*|^2} \prod_{s=2N_1+k_2+1}^{2N_1+N_2} \frac{|p_s - p_{2N_1+k_2}|^2}{|p_{2N_1+k_2} + p_s^*|^2} \right), \\
\widehat{\Omega}_{k_2}^+ &= \ln \left[\frac{1}{p_{2N_1+k_2} + p_{2N_1+k_2}^*} \left(\prod_{s=1}^{N_1} \prod_{s=2N_1+1}^{2N_1+k_2-1} \right) \frac{|p_s - p_{2N_1+k_2}|^2}{|p_{2N_1+k_2} + p_s^*|^2} \right].
\end{aligned} \tag{77}$$

From the explicit expressions of $\bar{\delta}_n^{(k_1)\pm}$ and $\bar{\delta}_n^{(2N_1+k_2)\pm}$ given in Eqs. (74) and (76), we obtain the asymptotic forms of the two distinct types of dark solitons in solution (3) for $N_1 N_2 \neq 0$ and $\max\{N_1, N_2\} \geq 2$, as stated in the following theorem.

Theorem 4. *As $t \rightarrow \pm\infty$ and under the velocity condition assumed in Eq. (62), the asymptotic expressions for the two types of dark soliton in mixed soliton solution (3) with $N_1 N_2 \neq 0$ and $\max\{N_1, N_2\} \geq 2$ are:*

- Along $\zeta_k \simeq \mathcal{O}(1)$, the asymptotic expression of the type-I dark soliton \mathbf{S}_{k_1} is

$$u_{k_1}^\pm \simeq \frac{\tilde{\chi}_{k_1}^{(1)\pm} + \tilde{\Theta}_{k_1}^{(1)\pm} \cosh(\zeta_{k_1} + \tilde{\Omega}_{k_1}^\pm)}{\tilde{\chi}_{k_1}^{(0)\pm} + \tilde{\Theta}_{k_1}^{(0)\pm} \cosh(\zeta_{k_1} + \tilde{\Omega}_{k_1}^\pm)}, \tag{78}$$

Here, $k_1 = 1, 2, \dots, N_1$.

- Along $\zeta_{2N_1+k_2} \simeq \mathcal{O}(1)$, the asymptotic expression of the type-II dark soliton $\bar{\mathbf{S}}_{k_2}$ is

$$\bar{u}_{k_2}^\pm \simeq \frac{1}{2} \widehat{\mu}_{k_2}^\pm \left[(1 + \widehat{y}_{k_2}) + (\widehat{y}_{k_2} - 1) \tanh\left(\frac{\zeta_{2N_1+k_2} + \widehat{\Omega}_{k_2}^\pm}{2}\right) \right], \tag{79}$$

Here, $k_2 = 1, 2, \dots, N_2$. Therefore, using the asymptotics for both types of dark solitons in Eqs. (78) and (79), the asymptotics of the general mixed dark soliton solution (3) with $N_1 N_2 \neq 0$ and $\max\{N_1, N_2\} \geq 2$ is given by

$$|u^\pm| \simeq \sum_{k_1=1}^{N_1} |u_{k_1}^\pm| + \sum_{k_2=1}^{N_2} |\bar{u}_{k_2}^\pm| - (N_1 + N_2 - 1). \tag{80}$$

Next, we provide some comments on these mixed-type soliton collisions based on the asymptotic expressions of Eqs. (78) and (79). First, the phase shifts experienced by the type-I dark soliton \mathbf{S}_{k_1} and the type-II dark soliton $\bar{\mathbf{S}}_{k_2}$, denoted as $\Delta\tilde{\Phi}_{k_1}$ and $\Delta\widehat{\Phi}_{k_2}$ respectively, are given by:

$$\begin{aligned}
\Delta\tilde{\Phi}_{k_1} &= \tilde{\Omega}_{k_1}^+ - \tilde{\Omega}_{k_1}^-, \\
\Delta\widehat{\Phi}_{k_2} &= \widehat{\Omega}_{k_2}^+ - \widehat{\Omega}_{k_2}^-.
\end{aligned} \tag{81}$$

The sum of phase shifts of all the type-I dark solitons and type-II dark solitons admits the relations

$$2 \left(\sum_{k_1=1}^{N_1} \Delta\tilde{\Phi}_{k_1} \right) + \left(\sum_{k_2=1}^{N_2} \Delta\widehat{\Phi}_{k_2} \right) = 0. \tag{82}$$

Second, it is confirmed that $|u_{k_1}^+(\zeta_{k_1})| \neq |u_{k_1}^-(\zeta_{k_1} + \Delta\tilde{\Phi}_{k_1})|$, while $|\bar{u}_{k_2}^+(\zeta_{2N_1+k_2})| = |\bar{u}_{k_2}^-(\zeta_{2N_1+k_2} + \Delta\widehat{\Phi}_{k_2})|$. Thus, the shapes of all type-I dark solitons $\mathbf{S}_1, \dots, \mathbf{S}_{N_1}$ change after the collisions, whereas the shapes of all type-II dark

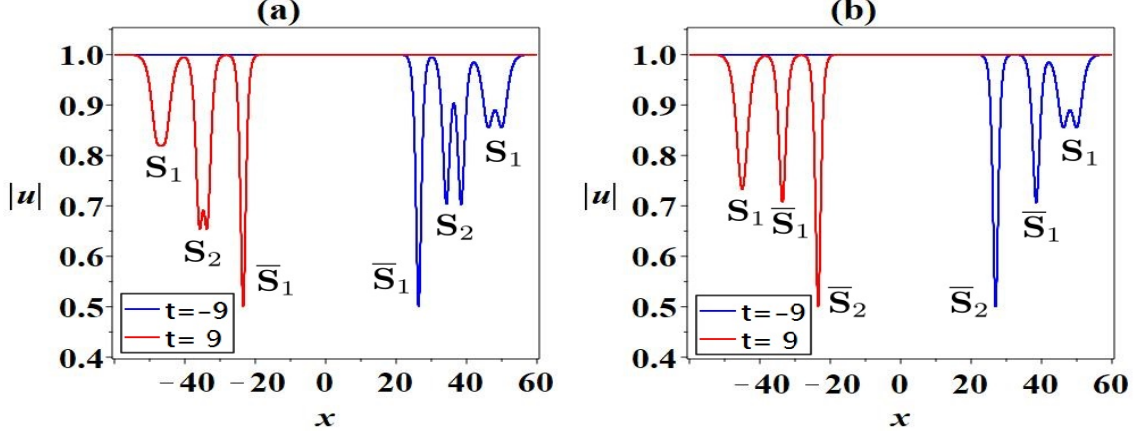


FIG. 11. (a) The shape-altering collisions of two type-I dark solitons and a type-II dark soliton with $(N_1, N_2) = (2, 1)$, $(p_1, p_2, p_5) = (e^{\frac{1}{3}i\pi}, e^{\frac{1}{4}i\pi}, e^{\frac{1}{6}i\pi})$ and $(\zeta_{1,0}, \zeta_{2,0}, \zeta_{5,0}) = (0, 0, 0)$. (b) The shape-altering collisions of one type-I dark soliton and two type-II dark solitons with $(N_1, N_2) = (1, 2)$, $(p_1, p_3, p_4) = (e^{\frac{1}{3}i\pi}, e^{\frac{1}{4}i\pi}, e^{\frac{1}{6}i\pi})$ and $(\zeta_{1,0}, \zeta_{3,0}, \zeta_{4,0}) = (0, 0, 0)$.

solitons $\bar{S}_1, \dots, \bar{S}_{N_2}$ remain unchanged. Consequently, collisions between mixed-type solitons are classified as shape-altering. Two typical examples are shown in Fig. 11: one involving two type-I and one type-II dark soliton, and the other involving one type-I and two type-II dark solitons. In both cases, we can directly observe that the shapes of the type-I dark solitons undergo significant changes, while the shapes of the type-II dark solitons remain unaffected.

Finally, we comment on the mutual influence between the two distinct types of solitons during collisions. Before proceeding, we need to emphasize that the pure type-I dark soliton S_{k_1} is determined by the parameter p_{k_1} , while the pure type-II dark soliton \bar{S}_{k_2} is controlled by the parameter $p_{2N_1+k_2}$.

We first consider the effect of type-I dark solitons on type-II dark solitons. Since the asymptotic expressions of the type-II soliton \bar{S}_{k_2} before and after the collision satisfy

$$|\bar{u}_{k_2}^+(\zeta_{2N_1+k_2})| = |\bar{u}_{k_2}^-(\zeta_{2N_1+k_2} + \Delta\hat{\Phi}_{k_2})|,$$

the parameter p_{k_1} associated with the type-I soliton affects only the phase shift $\Delta\hat{\Phi}_{k_2}$. This demonstrates that collisions with type-I solitons induce merely a phase shift in type-II solitons, while leaving their shapes and amplitudes unchanged.

Next, we consider the effects of type-II dark solitons on type-I dark solitons. This indicates that the inclusion of type-II dark solitons in the collisions indeed alters both the shapes and amplitudes of the type-I dark solitons. It is worth noting a key feature of the expressions $\tilde{\chi}_{k_1}^{(n)\pm}$ and $\tilde{\Theta}_{k_1}^{(n)\pm}$. As shown in Eq. (75) and the subsequent discussion, $\tilde{\chi}_{k_1}^{(n)-}$ and $\tilde{\Theta}_{k_1}^{(n)-}$ depend not only on the parameters p_1, p_2, \dots, p_{N_1} , but also on $p_{2N_1+1}, p_{2N_1+2}, \dots, p_{2N_1+N_2}$. In contrast, $\tilde{\chi}_{k_1}^{(n)+}$ and $\tilde{\Theta}_{k_1}^{(n)+}$ depend only on p_1, p_2, \dots, p_{N_1} , and are independent of $p_{2N_1+1}, p_{2N_1+2}, \dots, p_{2N_1+N_2}$. In other words,

$$\begin{aligned} \tilde{\chi}_{k_1}^{(n)-} &= \tilde{\chi}_{k_1}^{(n)-}(p_1, p_2, \dots, p_{N_1}, p_{2N_1+1}, p_{2N_1+2}, \dots, p_{2N_1+N_2}), \\ \tilde{\chi}_{k_1}^{(n)+} &= \tilde{\chi}_{k_1}^{(n)+}(p_1, p_2, \dots, p_{N_1}), \\ \tilde{\Theta}_{k_1}^{(n)-} &= \tilde{\Theta}_{k_1}^{(n)-}(p_1, p_2, \dots, p_{N_1}, p_{2N_1+1}, p_{2N_1+2}, \dots, p_{2N_1+N_2}), \\ \tilde{\Theta}_{k_1}^{(n)+} &= \tilde{\Theta}_{k_1}^{(n)+}(p_1, p_2, \dots, p_{N_1}). \end{aligned} \tag{83}$$

The specific expressions for the amplitude $\mathcal{I}_{k_1}^\pm$ of the type-I dark soliton S_{k_1} before and after the collisions are given by:

$$\mathcal{I}_{k_1}^\pm = |u_{k_1}^\pm| \Big|_{\zeta_{k_1} = -\tilde{\Omega}_{k_1}^\pm} = \left| \frac{\tilde{\chi}_{k_1}^{(1)\pm} + \tilde{\Theta}_{k_1}^{(1)\pm}}{\tilde{\chi}_{k_1}^{(0)\pm} + \tilde{\Theta}_{k_1}^{(0)\pm}} \right|. \tag{84}$$

Referring to Eq. (83), we conclude that $\mathcal{I}_{k_1}^-$ depends on the parameters $p_1, p_2, \dots, p_{N_1}, p_{2N_1+1}, p_{2N_1+2}, \dots, p_{2N_1+N_2}$, while $\mathcal{I}_{k_1}^+$ depends only on p_1, p_2, \dots, p_{N_1} . Specifically,

$$\begin{aligned}\mathcal{I}_{k_1}^- &= \mathcal{I}_{k_1}^-(p_1, p_2, \dots, p_{N_1}, p_{2N_1+1}, p_{2N_1+2}, \dots, p_{2N_1+N_2}), \\ \mathcal{I}_{k_1}^+ &= \mathcal{I}_{k_1}^+(p_1, p_2, \dots, p_{N_1}).\end{aligned}\quad (85)$$

Since the type-II dark solitons are characterized by the parameters $p_{2N_1+k_2}$, it follows from Eq. (85) that the type-II dark solitons only influence the amplitudes of the type-I soliton before the collision, while they have no effect on the amplitudes of the type-I soliton after the collision. As noted specifically below Eq. (75), $\tilde{\chi}_{k_1}^{(n)+} = \chi_{k_1}^{(n)}$ and $\tilde{\Theta}_{k_1}^{(n)+} = \Theta_{k_1}^{(n)}$, thus, the amplitude expressions $\mathcal{I}_{k_1}^+$ and \mathcal{I}_{k_1} in Eq. (61) satisfy the relation $\mathcal{I}_{k_1}^+ = \mathcal{I}_{k_1}$. This indicates that, in mixed soliton solutions, the amplitude of the type-I dark soliton \mathbf{S}_{k_1} is equal to that in the pure type-I dark soliton solutions, which further confirms that the influence of the type-II dark solitons on the amplitudes of the type-I dark solitons vanishes after their collisions.

Using a similar analytical approach, we conclude that the influence of type-II dark solitons on the shapes of type-I dark solitons also vanishes after their collisions. In particular, the shape of the type-I dark soliton \mathbf{S}_{k_1} before and after the collisions can be characterized by the factor $\tilde{\Delta}_{k_1}^\pm$, where

$$\tilde{\Delta}_{k_1}^\pm = [\partial_{\zeta_{k_1} \zeta_{k_1}} |u_{k_1}^\pm(\zeta_{k_1})|] \Big|_{\zeta_{k_1} = -\tilde{\Omega}_{k_1}^\pm}, \quad k_1 = 1, 2, \dots, N_1. \quad (86)$$

It follows that $\tilde{\Delta}_{k_1}^- = \tilde{\Delta}_{k_1}^-(p_1, p_2, \dots, p_{N_1}, p_{2N_1+1}, p_{2N_1+2}, \dots, p_{2N_1+N_2})$, whereas $\tilde{\Delta}_{k_1}^+ = \tilde{\Delta}_{k_1}^+(p_1, p_2, \dots, p_{N_1})$. Hence, the parameters $p_{2N_1+1}, p_{2N_1+2}, \dots, p_{2N_1+N_2}$ can affect the sign of $\tilde{\Delta}_{k_1}^-$ but have no influence on the sign of $\tilde{\Delta}_{k_1}^+$. This reveals that the type-II dark solitons can modify the shapes of the type-I dark solitons only before the collision, but not after it. In fact, the expression for $\tilde{\Delta}_{k_1}^+$ coincides with the shape factor $\tilde{\Delta}_{k_1}$ of the pure type-I dark solitons given in Eq. (60). Consequently, the shapes of the type-I dark solitons in the mixed soliton solutions are restored to those of the pure type-I dark soliton solutions after the collisions.

To provide a clearer visual understanding of the influence of type-II dark solitons on type-I dark solitons, we present two distinct cases of collisions between two type-I dark solitons and a single type-II dark soliton, together with a comparison to the collision of two pure type-I dark solitons, as shown in Fig. 12. In the three panels of this figure, even though the parameters p_1, p_2 that determine the identities of the two type-I dark solitons $\mathbf{S}_1, \mathbf{S}_2$ are identical, the two solitons nevertheless exhibit clearly distinct shapes and amplitudes before the collision, as indicated by the blue solid lines at $t = -8$. Specifically, changing the value of p_3 , which corresponds to modifying the properties of the type-II soliton $\bar{\mathbf{S}}_1$, also alters the shapes of the two type-I solitons \mathbf{S}_1 and \mathbf{S}_2 . Both cases indicate that the inclusion of the type-II dark soliton $\bar{\mathbf{S}}_1$ indeed causes alterations in the shapes and amplitudes of the two type-I dark solitons $\mathbf{S}_1, \mathbf{S}_2$. However, after the collision, these two type-I dark solitons share the same shapes and amplitudes as the pure two type-I dark solitons in panel (c), even though they collide with different single type-II dark solitons in panels (a) and (b), as shown by the red solid lines at $t = 8$ in all three panels. This indicates that the influence of the single type-II dark soliton on the two type-I dark solitons vanishes, even though the features of the single type-II dark soliton in panels (a) and (b) are distinct.

V. CONCLUSION

In this paper, we have derived general dark soliton solutions for the complex modified Korteweg–de Vries equation, expressed in terms of block determinants. The obtained general dark soliton solutions are classified into two distinct types, namely type-I and type-II dark solitons by assigning specific values to the sub-block orders in these determinant solutions. Strikingly, the single soliton of these two types differ not only in their mathematical structures but also in their three dynamical properties: (i) The single type-I dark soliton experiences no phase shift as x varies from $-\infty$ to $+\infty$, whereas the phase of the single type-II dark soliton shifts by $(\pi + 2\vartheta_1)$ over the same range. Here ϑ_1 is correlated to the soliton velocity through Eq. (16). (ii) The type-I dark soliton displays three distinct valley profiles: double-valley, single-valley, and flat-bottom (see Fig. 2), while the type-II dark soliton only exhibits a single-valley profile. (iii) The velocity-amplitude relations in these two types of dark solitons are distinct, as shown in Fig. 3. Notably, the valley profiles of a single type-I dark soliton are correlated with its velocity, as illustrated in detail in Fig. 1(c).

Further, collisions of multiple pure type-I dark solitons and collisions of multiple pure type-II dark solitons are shape-preserving, which do not change the soliton identities except for certain phase shifts. A rarely reported soliton phenomenon has been discovered in the collisions of multiple pure type-I dark solitons, where these multiple dark

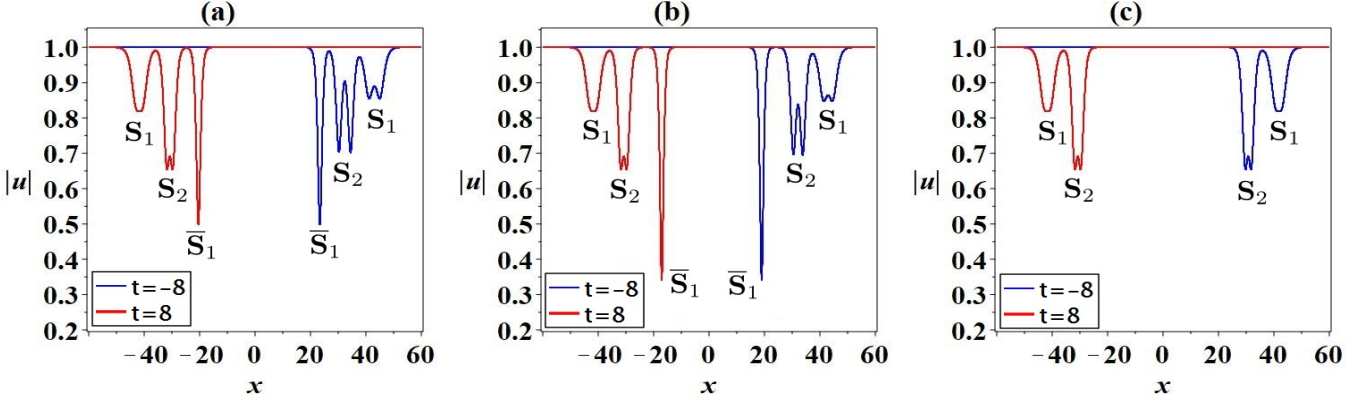


FIG. 12. (a) The mixed solutions (3) composed of two type-I dark solitons and a single type-II dark soliton with $(N_1, N_2) = (2, 1)$, $(p_1, p_2, p_5) = (e^{\frac{1}{3}i\pi}, e^{\frac{1}{4}i\pi}, e^{\frac{1}{6}i\pi})$ and $(\zeta_{1,0}, \zeta_{2,0}, \zeta_{5,0}) = (0, 0, 0)$; (b) The mixed solutions (3) composed of two type-I dark solitons and a single type-II dark soliton with $(N_1, N_2) = (2, 1)$, $(p_1, p_2, p_5) = (e^{\frac{1}{3}i\pi}, e^{\frac{1}{4}i\pi}, e^{\frac{1}{6}i\pi})$ and $(\zeta_{1,0}, \zeta_{2,0}, \zeta_{5,0}) = (0, 0, 0)$; (c) The pure two type-I dark soliton solutions (3) with $(N_1, N_2) = (2, 0)$, $(p_1, p_2) = (e^{\frac{1}{3}i\pi}, e^{\frac{1}{4}i\pi})$ and $(\zeta_{1,0}, \zeta_{2,0}) = (0, 0)$.

solitons mutually influence soliton properties of each other. Specifically, changing the velocity or other characteristics of one soliton can result in changes to the properties of all other type-I dark solitons, including their shapes and amplitudes. For instance, as shown in Fig. 5, in the collision scenario of two type-I dark solitons, denoted as \mathbf{S}_1 and \mathbf{S}_2 , we keep the parameters related to the properties of one soliton unchanged. However, its amplitude still exhibits noticeable changes as the velocity of the other soliton varies, even though the two solitons consistently undergo shape-preserving collisions. This unique characteristic is more intuitively observed in Fig. 7, where the valley profiles of soliton \mathbf{S}_2 clearly alter as the velocity of soliton \mathbf{S}_1 varies, even though the parameters related to the velocity of soliton \mathbf{S}_2 remain fixed. In contrast, multiple pure type-II dark solitons display completely different properties. They behave independently and only undergo phase shifts, without any further influence. Specifically, varying the velocity of one soliton does not affect the shapes or amplitudes of the other type-II solitons.

The coherent structures of type-I dark solitons with type-II dark solitons exhibit shape-altering collisions, resulting in significant changes to the properties of the type-I dark solitons, including their shapes and amplitudes. In contrast, the type-II dark solitons experience only phase shifts without any other changes in their shapes and amplitudes. More uniquely, the influence of type-II dark solitons on the shape alteration of type-I dark solitons exists only before the interaction. After the collision, this shape-altering effect disappears, and the shapes of the type-I dark solitons return to the form observed in the pure type-I dark soliton scenario, as if the type-II dark solitons were absent. Two specific examples demonstrating this shape-altering collision are shown in Fig. 9 and Fig. 12, where it can be visually observed that, prior to the collision, the shapes of the type-I dark solitons indeed vary with changes in the properties of the type-II dark solitons (see the plots at $t = -6$ in Fig. 9 and $t = -8$ in Fig. 12). However, after the collisions, this shape-altering effect disappears, and the shapes of the type-I dark solitons remain consistent (see the plots at $t = 6$ in Fig. 9 and $t = 8$ in Fig. 12). This unique type of shape-altering behavior in dark soliton collisions has rarely been reported before. This study will give impetus into the understanding of non-trivial multiple soliton collision behaviour in spinor condensates and in multi-mode optical fibers with intricate four-wave mixing.

Appendix A: Derivations of the general multiple dark soliton solutions

This appendix provides the detailed derivations of the multiple dark soliton solutions for the cmKdV equation as presented in Theorem 1.

Using Eq. (3), the cmKdV equation (2) can be transformed into the following bilinear form[40]:

$$\begin{aligned} (D_t + D_x^3 - 6D_x) g \cdot f &= 0, \\ (D_x^2 - 2) f \cdot f &= -2|g|^2, \end{aligned} \tag{A1}$$

where $f \in \mathbb{R}, g \in \mathbb{C}$. As confirmed in [44, 45], the bilinear equations:

$$\begin{aligned} (D_{x_1} D_{x_{-1}} - 2) \tau_n \cdot \tau_n &= -2\tau_{n+1}\tau_{n-1}, \\ (D_{x_{-1}}(D_{x_1}^2 - D_{x_2}) - 4D_{x_1}) \tau_{n+1} \cdot \tau_n &= 0, \\ (D_{x_1}^3 - 4D_{x_3} + 3D_{x_1}D_{x_2}) \tau_{n+1} \cdot \tau_n &= 0, \end{aligned} \quad (\text{A2})$$

admit tau functions of the form

$$\tau_n = \det_{1 \leq i, j \leq N} \left(m_{i,j}^{(n)} \right), \quad (\text{A3})$$

where $m_{i,j}^{(n)}$ is defined through a set of differential relations involving the functions $\Phi_i^{(n)}$ and $\bar{\Phi}_j^{(n)}$ as follows:

$$\begin{cases} \partial_{x_1} m_{i,j}^{(n)} = \Phi_i^{(n)} \bar{\Phi}_j^{(n)}, \partial_{x_{-1}} m_{i,j}^{(n)} = -\Phi_i^{(n-1)} \bar{\Phi}_j^{(n+1)}, \\ \partial_{x_2} m_{i,j}^{(n)} = \Phi_i^{(n+1)} \bar{\Phi}_j^{(n)} + \Phi_i^{(n)} \bar{\Phi}_j^{(n-1)}, \\ \partial_{x_3} m_{i,j}^{(n)} = \Phi_i^{(n+2)} \bar{\Phi}_j^{(n)} + \Phi_i^{(n+1)} \bar{\Phi}_j^{(n-1)} + \Phi_i^{(n)} \bar{\Phi}_j^{(n-2)}, \\ m_{i,j}^{(n+1)} = m_{i,j}^{(n)} + \Phi_i^{(n)} \bar{\Phi}_j^{(n+1)}, \end{cases} \quad (\text{A4})$$

with $\Phi_i^{(n)}$ and $\bar{\Phi}_j^{(n)}$ being arbitrary functions that satisfy:

$$\partial_{x_\ell} \Phi_i^{(n)} = \Phi_i^{(n+\ell)}, \partial_{x_\ell} \bar{\Phi}_j^{(n)} = -\bar{\Phi}_j^{(n-\ell)}, \ell = -1, 1, 2, 3. \quad (\text{A5})$$

A simple form for $\Phi_i^{(n)}$ and $\bar{\Phi}_j^{(n)}$, as satisfying Eq. (A5), is as follows:

$$\begin{aligned} \Phi_i^{(n)} &= p_i^n e^{\xi_i}, \xi_i = \frac{1}{p_i} x_{-1} + p_i x_1 + p_i^2 x_2 + p_i^3 x_3 + \xi_{i,0}, \\ \bar{\Phi}_j^{(n)} &= (-\bar{p}_j)^{-n} e^{\bar{\xi}_j}, \bar{\xi}_j = \frac{1}{\bar{p}_j} x_{-1} + \bar{p}_j x_1 - \bar{p}_j^2 x_2 + \bar{p}_j^3 x_3 + \bar{\xi}_{j,0}. \end{aligned} \quad (\text{A6})$$

Using such forms of $\Phi_i^{(n)}$ and $\bar{\Phi}_j^{(n)}$, we can express $m_{i,j}^{(n)}$ satisfying Eq. (A4) as:

$$m_{i,j}^{(n)} = \delta_{i,j} + \frac{1}{p_i + \bar{p}_j} \left(-\frac{p_i}{\bar{p}_j} \right)^n e^{\xi_i + \bar{\xi}_j}, \quad (\text{A7})$$

where $\delta_{i,j} = 1$ when $i = j$ and $\delta_{i,j} = 0$ when $i \neq j$.

To reduce Eq. (A2) to Eq. (A1), we have to first impose the constraint

$$p_i \bar{p}_i = 1, \quad (\text{A8})$$

so that τ_n can satisfy the dimensional reduction condition:

$$(\partial_{x_1} - \partial_{x_{-1}}) \tau_n = 0. \quad (\text{A9})$$

With this condition, x_{-1} in Eq. (A2) can be replaced by x_1 . After performing a simple linear substitution, the terms involving x_{-1} and x_2 in Eq. (A2) disappear, reducing Eq. (A2) to the following form:

$$\begin{aligned} (D_{x_1}^2 - 2) \tau_n \cdot \tau_n &= -2\tau_{n+1}\tau_{n-1}, \\ (D_{x_1}^3 - 3D_{x_1} - D_{x_3}) \tau_{n+1} \cdot \tau_n &= 0. \end{aligned} \quad (\text{A10})$$

Since this bilinear system is independent of x_{-1} and x_2 , we can set $x_{-1} = 0$ and $x_2 = 0$ in τ_n . Next, we impose $x_1, x_3 \in \mathbb{R}$ and the following conjugate constraint:

$$\bar{p}_i = p_i^*, \quad \bar{\xi}_{i,0} = \xi_{i,0}^*, \quad (\text{A11})$$

so that τ_n satisfies the condition:

$$\tau_n^* = \tau_{-n}. \quad (\text{A12})$$

If we further set $x_1 = x + 3t$, $x_3 = -t$, and $\tau_0 = f$, $\tau_1 = g$, $\tau_{-1} = g^*$, then Eq. (A10) reduces to Eq. (A1). Consequently, the solutions of the complex modified KdV (cmKdV) equation can be expressed through the tau functions as $u = \frac{\tau_1}{\tau_0}$.

Finally, by taking $N = 2N_1 + N_2$, $\zeta_i = \xi_i + \xi_i^*$, and imposing the parameter constraints in Eq. (7), the functions τ_n and $\bar{\delta}_n$ of Eq. (4) will admit the following correlation:

$$\tau_n = \mathcal{C}\bar{\delta}_n, \quad (\text{A13})$$

where $\mathcal{C} = \exp\left(\sum_{i=1}^{2N_1+N_2} \zeta_i\right)$. Since the factor \mathcal{C} can be canceled out without affecting the solution $u = \frac{\tau_1}{\tau_0} = \frac{\mathcal{C}\bar{\delta}_1}{\mathcal{C}\bar{\delta}_0}$, the solutions of the cmKdV equation in the form of Theorem 1 are derived.

Appendix B: The long-time asymptotic analysis to function $\bar{\delta}_n$

In this appendix, we will present the proofs of Lemma 1 and Lemma 2. The proof of Lemma 3 combines the results of Lemma 1 and Lemma 2 and is omitted for brevity. To begin with, we introduce the explicit form of the well-known Cauchy determinant through the following lemma.

Lemma 4. *Let $D_N = \det_{1 \leq s, j \leq N} \left(\frac{1}{a_s + b_j} \right)$ represent a Cauchy determinant with entries given by $\frac{1}{a_s + b_j}$. Then, it follows that $D_N = \frac{\prod_{1 \leq s < j \leq N} (a_j - a_s)(b_j - b_s)}{\prod_{s, j=1}^N (a_s + b_j)}$.*

Lemma 4 can be confirmed through fundamental determinant operations.

1. Proof of Lemma1

In order to prove Lemma 1, we start by reviewing the necessary preliminary conditions and assumptions associated with it. In this case, we examine the pure N_1 type-I dark soliton. The velocities of each soliton are defined as $\nu_{k_1} = 2\cos(2\vartheta_{k_1}) - 4$, $k_1 = 1, 2, \dots, N_1$. Here, $\vartheta_{k_1} \in (-\frac{\pi}{2}, \frac{\pi}{2})$, ensuring that $\nu_{k_1} \in (-6, -2]$. Without loss of generality, we assume

$$\nu_1 < \nu_2 < \dots < \nu_{k_1} < \dots < \nu_{N_1} < 0, \quad (\text{B1})$$

Given the symmetry condition $\zeta_{N_1+s} = -\zeta_s + i\pi$, we additionally obtain

$$\nu_{N_1+1} < \nu_{N_1+2} < \dots < \nu_{N_1+k_1} < \dots < \nu_{2N_1} < 0. \quad (\text{B2})$$

Considering these conditions, we can explore the asymptotic behaviors of $\bar{\delta}_n$ as $t \rightarrow \infty$ and $t \rightarrow -\infty$, respectively. The discussion is conducted around the neighbourhood of $\zeta_{k_1} \approx 0$, which implies $x \approx \nu_{k_1}t$.

(a) Before collision $t \rightarrow -\infty$

As $t \rightarrow -\infty$, the following results hold for e^{ζ_j} and $e^{-\zeta_j}$:

$$\begin{cases} e^{\zeta_j} \rightarrow \infty, & j > k_1, \\ e^{\zeta_j} \rightarrow 0, & j < k_1, \end{cases} \quad \text{and} \quad \begin{cases} e^{-\zeta_j} \rightarrow 0, & j > k_1, \\ e^{-\zeta_j} \rightarrow \infty, & j < k_1, \end{cases} \quad (\text{B3})$$

Next, we undertake the asymptotic analysis of the function $\bar{\delta}_n$. By examining the asymptotic properties of e^{ζ_j} and $e^{-\zeta_j}$ and applying the symmetry condition $\zeta_{N_1+s} = -\zeta_s + i\pi$, we derive the following asymptotic expression.

$$\begin{aligned}
\bar{\delta}_n &\simeq \bar{\delta}_n^{[k_1]-} \\
&= (-1)^{N_1-k_1} e^{-\sum_{s=1}^{k_1-1} \zeta_s + \sum_{s=k_1+1}^{N_1} \zeta_s} \times \\
&\quad \left| \begin{array}{cccccccccccc}
1 & \cdots & 0 & 0 & \cdots & 0 & 0 & \cdots & 0 & 0 & 0 & 0 & \cdots & 0 \\
\vdots & \ddots & \vdots & \vdots & \ddots & \vdots & \vdots & \ddots & \vdots & \vdots & \vdots & \vdots & \ddots & \vdots \\
0 & \cdots & 1 & 0 & \cdots & 0 & 0 & \cdots & 0 & 0 & 0 & 0 & \cdots & 0 \\
0 & \cdots & 0 & \bar{m}_{k_1, k_1}^{(n)} + e^{-\zeta_{k_1}} & \bar{m}_{k_1, k_1+1}^{(n)} & \cdots & \bar{m}_{k_1, N_1}^{(n)} & \bar{m}_{k_1, N_1+1}^{(n)} & \cdots & \bar{m}_{k_1, N_1+k_1-1}^{(n)} & \bar{m}_{k_1, N_1+k_1}^{(n)} & 0 & \cdots & 0 \\
0 & \cdots & 0 & \bar{m}_{k_1+1, k_1}^{(n)} & \bar{m}_{k_1+1, k_1+1}^{(n)} & \cdots & \bar{m}_{k_1+1, N_1}^{(n)} & \bar{m}_{k_1+1, N_1+1}^{(n)} & \cdots & \bar{m}_{k_1+1, N_1+k_1-1}^{(n)} & \bar{m}_{k_1+1, N_1+k_1}^{(n)} & 0 & \cdots & 0 \\
\vdots & \ddots & \vdots & \vdots & \ddots & \vdots & \vdots & \ddots & \vdots & \vdots & \vdots & \vdots & \ddots & \vdots \\
0 & \cdots & 0 & \bar{m}_{N_1, k_1}^{(n)} & \bar{m}_{N_1, k_1+1}^{(n)} & \cdots & \bar{m}_{N_1, N_1}^{(n)} & \bar{m}_{N_1, N_1+1}^{(n)} & \cdots & \bar{m}_{N_1, N_1+k_1-1}^{(n)} & \bar{m}_{N_1, N_1+k_1}^{(n)} & 0 & \cdots & 0 \\
0 & \cdots & 0 & \bar{m}_{N_1+1, k_1}^{(n)} & \bar{m}_{N_1+1, k_1+1}^{(n)} & \cdots & \bar{m}_{N_1+1, N_1}^{(n)} & \bar{m}_{N_1+1, N_1+1}^{(n)} & \cdots & \bar{m}_{N_1+1, N_1+k_1-1}^{(n)} & \bar{m}_{N_1+1, N_1+k_1}^{(n)} & 0 & \cdots & 0 \\
\vdots & \ddots & \vdots & \vdots & \ddots & \vdots & \vdots & \ddots & \vdots & \vdots & \vdots & \vdots & \ddots & \vdots \\
0 & \cdots & 0 & \bar{m}_{N_1+k_1-1, k_1}^{(n)} & \bar{m}_{N_1+k_1-1, k_1+1}^{(n)} & \cdots & \bar{m}_{N_1+k_1-1, N_1}^{(n)} & \bar{m}_{N_1+k_1-1, N_1+1}^{(n)} & \cdots & \bar{m}_{N_1+k_1-1, N_1+k_1-1}^{(n)} & \bar{m}_{N_1+k_1-1, N_1+k_1}^{(n)} & 0 & \cdots & 0 \\
0 & \cdots & 0 & \bar{m}_{N_1+k_1, k_1}^{(n)} & \bar{m}_{N_1+k_1, k_1+1}^{(n)} & \cdots & \bar{m}_{N_1+k_1, N_1}^{(n)} & \bar{m}_{N_1+k_1, N_1+1}^{(n)} & \cdots & \bar{m}_{N_1+k_1, N_1+k_1-1}^{(n)} & \bar{m}_{N_1+k_1, N_1+k_1}^{(n)} + e^{-\zeta_{N_1+k_1}} & 0 & \cdots & 0 \\
0 & \cdots & 0 & 0 & 0 & \cdots & 0 & 0 & \cdots & 0 & 0 & 0 & \cdots & 1 \\
\end{array} \right| \\
&= (-1)^{N_1-k_1} e^{-\sum_{s=1}^{k_1-1} \zeta_s + \sum_{s=k_1+1}^{N_1} \zeta_s} \times \mathcal{A} \tag{B4}
\end{aligned}$$

with

$$\mathcal{A} = \left| \begin{array}{cccccccc}
\bar{m}_{k_1, k_1}^{(n)} + e^{-\zeta_{k_1}} & \bar{m}_{k_1, k_1+1}^{(n)} & \cdots & \bar{m}_{k_1, N_1}^{(n)} & \bar{m}_{k_1, N_1+1}^{(n)} & \cdots & \bar{m}_{k_1, N_1+k_1-1}^{(n)} & \bar{m}_{k_1, N_1+k_1}^{(n)} \\
\bar{m}_{k_1+1, k_1}^{(n)} & \bar{m}_{k_1+1, k_1+1}^{(n)} & \cdots & \bar{m}_{k_1+1, N_1}^{(n)} & \bar{m}_{k_1+1, N_1+1}^{(n)} & \cdots & \bar{m}_{k_1+1, N_1+k_1-1}^{(n)} & \bar{m}_{k_1+1, N_1+k_1}^{(n)} \\
\vdots & \vdots & \ddots & \vdots & \vdots & \ddots & \vdots & \vdots \\
\bar{m}_{N_1, k_1}^{(n)} & \bar{m}_{N_1, k_1+1}^{(n)} & \cdots & \bar{m}_{N_1, N_1}^{(n)} & \bar{m}_{N_1, N_1+1}^{(n)} & \cdots & \bar{m}_{N_1, N_1+k_1-1}^{(n)} & \bar{m}_{N_1, N_1+k_1}^{(n)} \\
\bar{m}_{N_1+1, k_1}^{(n)} & \bar{m}_{N_1+1, k_1+1}^{(n)} & \cdots & \bar{m}_{N_1+1, N_1}^{(n)} & \bar{m}_{N_1+1, N_1+1}^{(n)} & \cdots & \bar{m}_{N_1+1, N_1+k_1-1}^{(n)} & \bar{m}_{N_1+1, N_1+k_1}^{(n)} \\
\vdots & \vdots & \ddots & \vdots & \vdots & \ddots & \vdots & \vdots \\
\bar{m}_{N_1+k_1-1, k_1}^{(n)} & \bar{m}_{N_1+k_1-1, k_1+1}^{(n)} & \cdots & \bar{m}_{N_1+k_1-1, N_1}^{(n)} & \bar{m}_{N_1+k_1-1, N_1+1}^{(n)} & \cdots & \bar{m}_{N_1+k_1-1, N_1+k_1-1}^{(n)} & \bar{m}_{N_1+k_1-1, N_1+k_1}^{(n)} + e^{-\zeta_{N_1+k_1}} \\
\bar{m}_{N_1+k_1, k_1}^{(n)} & \bar{m}_{N_1+k_1, k_1+1}^{(n)} & \cdots & \bar{m}_{N_1+k_1, N_1}^{(n)} & \bar{m}_{N_1+k_1, N_1+1}^{(n)} & \cdots & \bar{m}_{N_1+k_1, N_1+k_1-1}^{(n)} & \bar{m}_{N_1+k_1, N_1+k_1}^{(n)} + e^{-\zeta_{N_1+k_1}}
\end{array} \right| \tag{B5}$$

Using the linearity of the determinant, we can express \mathcal{A} as the sum of four separate determinants:

$$\mathcal{A} = \mathcal{A}_1 + \mathcal{A}_2 + \mathcal{A}_3 + \mathcal{A}_4. \tag{B6}$$

Here,

With Eq. (6) and Lemma 4, one can find the following results.

$$\begin{aligned} \mathcal{A}_1 &= \prod_{s=k_1}^{N_1+k_1} \left(-\frac{p_s}{p_s^*} \right)^n \mathcal{D}_{[k_1, N_1+k_1]}, & \mathcal{A}_2 &= \prod_{s=k_1+1}^{N_1+k_1} \left(-\frac{p_s}{p_s^*} \right)^n e^{-\zeta_{k_1}} \mathcal{D}_{[k_1+1, N_1+k_1]}, \\ \mathcal{A}_3 &= \prod_{s=k_1}^{N_1+k_1-1} \left(-\frac{p_s}{p_s^*} \right)^n e^{-\zeta_{N_1+k_1}} \mathcal{D}_{[k_1, N_1+k_1-1]}, & \mathcal{A}_4 &= - \prod_{s=k_1+1}^{N_1+k_1-1} \left(-\frac{p_s}{p_s^*} \right)^n \mathcal{D}_{[k_1+1, N_1+k_1-1]}. \end{aligned} \tag{B8}$$

The explicit expression of \mathcal{A} can be display as:

$$\begin{aligned}
\mathcal{A} = & \mathcal{D}_{[k_1+1, N_1+k_1-1]} \prod_{s=k_1+1}^{N_1+k_1-1} \left(-\frac{p_s}{p_s^*} \right)^n \\
& \times \left[\left(-\frac{p_{k_1}}{p_{k_1}^*} \right)^{2n} \frac{4}{|p_{k_1} - p_{k_1}^*|^2} \frac{(-1)}{|p_{k_1} + p_{k_1}^*|^2} \left(\prod_{s=1}^{k_1-1} \prod_{k_1+1}^{N_1} \right) \frac{|p_{k_1} + p_s|^2}{|p_s - p_{k_1}^*|^2} \frac{|p_{k_1} - p_s|^2}{|p_s + p_{k_1}^*|^2} \right. \\
& + \left(-\frac{p_{k_1}}{p_{k_1}^*} \right)^n e^{-\zeta_{k_1}} \frac{-1}{p_{k_1} + p_{k_1}^*} \prod_{s=1}^{k_1-1} \frac{|p_{k_1} - p_s|^2}{|p_s + p_{k_1}^*|^2} \prod_{s=k_1+1}^{N_1} \frac{|p_{k_1} + p_s|^2}{|p_s - p_{k_1}^*|^2} \\
& - \left. \left(-\frac{p_{k_1}}{p_{k_1}^*} \right)^n e^{+\zeta_{k_1}} \frac{1}{p_{k_1} + p_{k_1}^*} \prod_{s=1}^{k_1-1} \frac{|p_{k_1} + p_s|^2}{|p_s - p_{k_1}^*|^2} \prod_{s=k_1+1}^{N_1} \frac{|p_{k_1} - p_s|^2}{|p_s + p_{k_1}^*|^2} - 1 \right] \\
= & \mathcal{D}_{[k_1+1, N_1+k_1-1]} \left[\chi_{k_1}^{(n)} + \Theta_{k_1}^{(n)} \cosh(\zeta_{k_1} + \Omega_{k_1}) \right].
\end{aligned} \tag{B9}$$

(b) After collision $t \rightarrow \infty$

As $t \rightarrow +\infty$, the following results hold for e^{ζ_j} and $e^{-\zeta_j}$:

$$\begin{cases} e^{\zeta_j} \rightarrow 0, & j > k_1, \\ e^{\zeta_j} \rightarrow \infty, & j < k_1. \end{cases} \quad \text{and} \quad \begin{cases} e^{-\zeta_j} \rightarrow \infty, & j > k_1, \\ e^{-\zeta_j} \rightarrow 0, & j < k_1. \end{cases} \tag{B10}$$

By examining the asymptotic properties of e^{ζ_j} and $e^{-\zeta_j}$ and applying the symmetry condition $\zeta_{N_1+s} = -\zeta_s + i\pi$, we derive the following asymptotic expression of $\bar{\delta}_n$.

$$\begin{aligned}
\bar{\delta}_n \simeq & \bar{\delta}_n^{[k_1]+} \\
= & (-1)^{k_1-1} e^{\sum_{s=1}^{k_1-1} \zeta_s - \sum_{s=k_1+1}^{N_1} \zeta_s} \times \\
& \left| \begin{array}{ccccccccccccc} \bar{m}_{1,1}^{(n)} & \cdots & \bar{m}_{1,k_1-1}^{(n)} & \bar{m}_{1,k_1}^{(n)} & 0 & \cdots & 0 & 0 & \cdots & 0 & \bar{m}_{1,N_1+k_1}^{(n)} & \bar{m}_{1,N_1+k_1+1}^{(n)} & \cdots & \bar{m}_{1,2N_1}^{(n)} \\ \vdots & & \vdots & \vdots & \vdots & \ddots & \vdots & \vdots & \ddots & \vdots & \vdots & \vdots & \ddots & \vdots \\ \bar{m}_{k_1-1,1}^{(n)} & \cdots & \bar{m}_{k_1-1,k_1-1}^{(n)} + e^{-\zeta_{k_1-1}} & \bar{m}_{k_1-1,k_1}^{(n)} & 0 & \cdots & 0 & 0 & \cdots & 0 & \bar{m}_{k_1-1,N_1+k_1}^{(n)} & \bar{m}_{k_1-1,N_1+k_1+1}^{(n)} & \cdots & \bar{m}_{k_1-1,2N_1}^{(n)} \\ \bar{m}_{k_1,1}^{(n)} & \cdots & \bar{m}_{k_1,k_1-1}^{(n)} & \bar{m}_{k_1,k_1}^{(n)} + e^{-\zeta_{k_1}} & 0 & \cdots & 0 & 0 & \cdots & 0 & \bar{m}_{k_1,N_1+k_1}^{(n)} & \bar{m}_{k_1,N_1+k_1+1}^{(n)} & \cdots & \bar{m}_{k_1,2N_1}^{(n)} \\ 0 & \cdots & 0 & 0 & 1 & \cdots & 0 & 0 & \cdots & 0 & 0 & 0 & \cdots & 0 \\ \vdots & & \vdots & \vdots & \vdots & \ddots & \vdots & \vdots & \ddots & \vdots & \vdots & \vdots & \ddots & \vdots \\ 0 & \cdots & 0 & 0 & 0 & \cdots & 1 & 0 & \cdots & 1 & 0 & 0 & \cdots & 0 \\ 0 & \cdots & 0 & 0 & 0 & \cdots & 0 & 0 & \cdots & 0 & 0 & 0 & \cdots & 0 \\ \vdots & & \vdots & \vdots & \vdots & \ddots & \vdots & \vdots & \ddots & \vdots & \vdots & \vdots & \ddots & \vdots \\ 0 & \cdots & 0 & 0 & 0 & \cdots & 1 & 0 & \cdots & 0 & 0 & 0 & \cdots & 0 \\ \bar{m}_{N_1+k_1,1}^{(n)} & \cdots & \bar{m}_{N_1+k_1,k_1-1}^{(n)} & \bar{m}_{N_1+k_1,k_1}^{(n)} & 0 & \cdots & 0 & 0 & \cdots & 0 & \bar{m}_{N_1+k_1,N_1+k_1}^{(n)} + e^{-\zeta_{N_1+k_1}} & \bar{m}_{N_1+k_1,N_1+k_1+1}^{(n)} & \cdots & \bar{m}_{N_1+k_1,2N_1}^{(n)} \\ \bar{m}_{N_1+k_1+1,1}^{(n)} & \cdots & \bar{m}_{N_1+k_1+1,k_1-1}^{(n)} & \bar{m}_{N_1+k_1+1,k_1}^{(n)} & 0 & \cdots & 0 & 0 & \cdots & 0 & \bar{m}_{N_1+k_1+1,N_1+k_1}^{(n)} & \bar{m}_{N_1+k_1+1,N_1+k_1+1}^{(n)} & \cdots & \bar{m}_{N_1+k_1+1,2N_1}^{(n)} \\ \vdots & & \vdots & \vdots & \vdots & \ddots & \vdots & \vdots & \ddots & \vdots & \vdots & \vdots & \ddots & \vdots \\ \bar{m}_{2N_1,1}^{(n)} & \cdots & \bar{m}_{2N_1,k_1-1}^{(n)} & \bar{m}_{2N_1,k_1}^{(n)} & 0 & \cdots & 0 & 0 & \cdots & 0 & \bar{m}_{2N_1,N_1+k_1}^{(n)} & \bar{m}_{2N_1,N_1+k_1+1}^{(n)} & \cdots & \bar{m}_{2N_1,2N_1}^{(n)} \end{array} \right| \\
= & (-1)^{k_1-1} e^{\sum_{s=1}^{k_1-1} \zeta_s - \sum_{s=k_1+1}^{N_1} \zeta_s} \times \\
& \left| \begin{array}{ccccccccccccc} \bar{m}_{1,1}^{(n)} & \cdots & \bar{m}_{1,k_1-1}^{(n)} & \bar{m}_{1,k_1}^{(n)} & \bar{m}_{1,N_1+k_1}^{(n)} & \bar{m}_{1,N_1+k_1+1}^{(n)} & \cdots & \bar{m}_{1,2N_1}^{(n)} \\ \vdots & & \vdots & \vdots & \vdots & \vdots & \ddots & \vdots \\ \bar{m}_{k_1-1,1}^{(n)} & \cdots & \bar{m}_{k_1-1,k_1-1}^{(n)} + e^{-\zeta_{k_1-1}} & \bar{m}_{k_1-1,k_1}^{(n)} & \bar{m}_{k_1-1,N_1+k_1}^{(n)} & \bar{m}_{k_1-1,N_1+k_1+1}^{(n)} & \cdots & \bar{m}_{k_1-1,2N_1}^{(n)} \\ \bar{m}_{k_1,1}^{(n)} & \cdots & \bar{m}_{k_1,k_1-1}^{(n)} & \bar{m}_{k_1,k_1}^{(n)} + e^{-\zeta_{k_1}} & \bar{m}_{k_1,N_1+k_1}^{(n)} & \bar{m}_{k_1,N_1+k_1+1}^{(n)} & \cdots & \bar{m}_{k_1,2N_1}^{(n)} \\ \bar{m}_{N_1+k_1,1}^{(n)} & \cdots & \bar{m}_{N_1+k_1,k_1-1}^{(n)} & \bar{m}_{N_1+k_1,k_1}^{(n)} & \bar{m}_{N_1+k_1,N_1+k_1}^{(n)} + e^{-\zeta_{N_1+k_1}} & \bar{m}_{N_1+k_1,N_1+k_1+1}^{(n)} & \cdots & \bar{m}_{N_1+k_1,2N_1}^{(n)} \\ \bar{m}_{N_1+k_1+1,1}^{(n)} & \cdots & \bar{m}_{N_1+k_1+1,k_1-1}^{(n)} & \bar{m}_{N_1+k_1+1,k_1}^{(n)} & \bar{m}_{N_1+k_1+1,N_1+k_1}^{(n)} & \bar{m}_{N_1+k_1+1,N_1+k_1+1}^{(n)} & \cdots & \bar{m}_{N_1+k_1+1,2N_1}^{(n)} \\ \vdots & & \vdots & \vdots & \vdots & \vdots & \ddots & \vdots \\ \bar{m}_{2N_1,1}^{(n)} & \cdots & \bar{m}_{2N_1,k_1-1}^{(n)} & \bar{m}_{2N_1,k_1}^{(n)} & \bar{m}_{2N_1,N_1+k_1}^{(n)} & \bar{m}_{2N_1,N_1+k_1+1}^{(n)} & \cdots & \bar{m}_{2N_1,2N_1}^{(n)} \end{array} \right|, t \rightarrow -\infty. \tag{B11}
\end{aligned}$$

Using a similar approach as presented above for the case where $t \rightarrow -\infty$, we can obtain the explicit asymptotic expression for $\bar{\delta}_n$ as $t \rightarrow \infty$, thus completing the proof of Lemma 1.

2. Proof of Lemma 2

In Lemma 2, we discuss the pure N_2 type-II dark soliton and assume that the velocities satisfy the following constraint:

$$\bar{\nu}_1 < \bar{\nu}_2 < \cdots < \bar{\nu}_{k_2} < \cdots < \bar{\nu}_{N_2} < 0. \quad (\text{B12})$$

The discussion is conducted around the neighbourhood of $\zeta_{k_2} \approx 0$, which implies $x \approx \bar{\nu}_{k_2} t$.

(a) Before collision $t \rightarrow -\infty$

We have

$$\begin{cases} e^{-\zeta_j} \rightarrow 0, & j > k_2, \\ e^{-\zeta_j} \rightarrow \infty, & j < k_2. \end{cases} \quad (\text{B13})$$

The asymptotic expression of $\bar{\delta}_n$ is derived as

$$\begin{aligned} \bar{\delta}_n &= \begin{vmatrix} \bar{m}_{1,1}^{(n)} + e^{-\zeta_1} & \cdots & \bar{m}_{1,k_2-1}^{(n)} & \bar{m}_{1,k_2}^{(n)} & \bar{m}_{1,k_2+1}^{(n)} & \cdots & \bar{m}_{1,N_2}^{(n)} \\ \vdots & \ddots & \vdots & \vdots & \vdots & \ddots & \vdots \\ \bar{m}_{k_2-1,1}^{(n)} & \cdots & \bar{m}_{k_2-1,k_2-1}^{(n)} + e^{-\zeta_{k_2-1}} & \bar{m}_{k_2-1,k_2}^{(n)} & \bar{m}_{k_2-1,k_2+1}^{(n)} & \cdots & \bar{m}_{k_2-1,N_2}^{(n)} \\ \bar{m}_{k_2,1}^{(n)} & \cdots & \bar{m}_{k_2,k_2-1}^{(n)} & \bar{m}_{k_2,k_2}^{(n)} + e^{-\zeta_{k_2}} & \bar{m}_{k_2,k_2+1}^{(n)} & \cdots & \bar{m}_{k_2,N_2}^{(n)} \\ \bar{m}_{k_2+1,1}^{(n)} & \cdots & \bar{m}_{k_2+1,k_2-1}^{(n)} & \bar{m}_{k_2+1,k_2}^{(n)} & \bar{m}_{k_2+1,k_2+1}^{(n)} + e^{-\zeta_{k_2+1}} & \cdots & \bar{m}_{k_2+1,N_2}^{(n)} \\ \vdots & \ddots & \vdots & \vdots & \vdots & \ddots & \vdots \\ \bar{m}_{N_2,1}^{(n)} & \cdots & \bar{m}_{N_2,k_2-1}^{(n)} & \bar{m}_{N_2,k_2}^{(n)} & \bar{m}_{N_2,k_2+1}^{(n)} & \cdots & \bar{m}_{N_2,N_2}^{(n)} + e^{-\zeta_{N_2}} \end{vmatrix} \\ &\simeq \bar{\delta}_n^{[k_2]-} \\ &= e^{-\sum_{s=1}^{k_2-1} \zeta_s} \times \begin{vmatrix} 1 & \cdots & 0 & 0 & 0 & \cdots & 0 \\ \vdots & \ddots & \vdots & \vdots & \vdots & \ddots & \vdots \\ 0 & \cdots & 1 & 0 & 0 & \cdots & 0 \\ 0 & \cdots & 0 & \bar{m}_{k_2,k_2}^{(n)} + e^{-\zeta_{k_2}} & \bar{m}_{k_2,k_2+1}^{(n)} & \cdots & \bar{m}_{k_2,N_2}^{(n)} \\ 0 & \cdots & 0 & \bar{m}_{k_2+1,k_2}^{(n)} & \bar{m}_{k_2+1,k_2+1}^{(n)} & \cdots & \bar{m}_{k_2+1,N_2}^{(n)} \\ \vdots & \ddots & \vdots & \vdots & \vdots & \ddots & \vdots \\ 0 & \cdots & 0 & \bar{m}_{N_2,k_2}^{(n)} & \bar{m}_{N_2,k_2+1}^{(n)} & \cdots & \bar{m}_{N_2,N_2}^{(n)} \end{vmatrix} \\ &= e^{-\sum_{s=1}^{k_2-1} \zeta_s} \times \left(\begin{vmatrix} e^{-\zeta_{k_2}} & 0 & \cdots & 0 \\ \bar{m}_{k_2+1,k_2}^{(n)} & \bar{m}_{k_2+1,k_2+1}^{(n)} & \cdots & \bar{m}_{k_2+1,N_2}^{(n)} \\ \vdots & \vdots & \ddots & \vdots \\ \bar{m}_{N_2,k_2}^{(n)} & \bar{m}_{N_2,k_2+1}^{(n)} & \cdots & \bar{m}_{N_2,N_2}^{(n)} \end{vmatrix} + \begin{vmatrix} \bar{m}_{k_2,k_2}^{(n)} & \bar{m}_{k_2,k_2+1}^{(n)} & \cdots & \bar{m}_{k_2,N_2}^{(n)} \\ \bar{m}_{k_2+1,k_2}^{(n)} & \bar{m}_{k_2+1,k_2+1}^{(n)} & \cdots & \bar{m}_{k_2+1,N_2}^{(n)} \\ \vdots & \vdots & \ddots & \vdots \\ \bar{m}_{N_2,k_2}^{(n)} & \bar{m}_{N_2,k_2+1}^{(n)} & \cdots & \bar{m}_{N_2,N_2}^{(n)} \end{vmatrix} \right), \quad t \rightarrow -\infty. \end{aligned}$$

(b) After collision $t \rightarrow \infty$
We have

$$\begin{cases} e^{-\zeta_j} \rightarrow \infty, & j > k_2, \\ e^{-\zeta_j} \rightarrow 0, & j < k_2. \end{cases} \quad (\text{B14})$$

The asymptotic expression of $\bar{\delta}_n$ is derived as

$$\begin{aligned}
\bar{\delta}_n &= \left| \begin{array}{cccccc} \bar{m}_{1,1}^{(n)} + e^{-\zeta_1} & \dots & \bar{m}_{1,k_2-1}^{(n)} & \bar{m}_{1,k_2}^{(n)} & \bar{m}_{1,k_2+1}^{(n)} & \dots & \bar{m}_{1,N_2}^{(n)} \\ \vdots & \ddots & \vdots & \vdots & \vdots & \ddots & \vdots \\ \bar{m}_{k_2-1,1}^{(n)} & \dots & \bar{m}_{k_2-1,k_2-1}^{(n)} + e^{-\zeta_{k_2-1}} & \bar{m}_{k_2-1,k_2}^{(n)} & \bar{m}_{k_2-1,k_2+1}^{(n)} & \dots & \bar{m}_{k_2-1,N_2}^{(n)} \\ \bar{m}_{k_2,1}^{(n)} & \dots & \bar{m}_{k_2,k_2-1}^{(n)} & \bar{m}_{k_2,k_2}^{(n)} + e^{-\zeta_{k_2}} & \bar{m}_{k_2,k_2+1}^{(n)} & \dots & \bar{m}_{k_2,N_2}^{(n)} \\ \bar{m}_{k_2+1,1}^{(n)} & \dots & \bar{m}_{k_2+1,k_2-1}^{(n)} & \bar{m}_{k_2+1,k_2}^{(n)} & \bar{m}_{k_2+1,k_2+1}^{(n)} + e^{-\zeta_{k_2+1}} & \dots & \bar{m}_{k_2+1,N_2}^{(n)} \\ \vdots & \ddots & \vdots & \vdots & \vdots & \ddots & \vdots \\ \bar{m}_{N_2,1}^{(n)} & \dots & \bar{m}_{N_2,k_2-1}^{(n)} & \bar{m}_{N_2,k_2}^{(n)} & \bar{m}_{N_2,k_2+1}^{(n)} & \dots & \bar{m}_{N_2,N_2}^{(n)} + e^{-\zeta_{N_2}} \end{array} \right| \\
&\simeq \bar{\delta}_n^{[k_2]} + \\
&= e^{-\sum_{s=k_2+1}^{N_2} \zeta_s} \times \left| \begin{array}{ccccc} \bar{m}_{1,1}^{(n)} & \dots & \bar{m}_{1,k_2-1}^{(n)} & \bar{m}_{1,k_2}^{(n)} & 0 \dots 0 \\ \vdots & \ddots & \vdots & \vdots & \vdots \ddots \vdots \\ \bar{m}_{k_2-1,1}^{(n)} & \dots & \bar{m}_{k_2-1,k_2-1}^{(n)} & \bar{m}_{k_2-1,k_2}^{(n)} & 0 \dots 0 \\ \bar{m}_{k_2,1}^{(n)} & \dots & \bar{m}_{k_2,k_2-1}^{(n)} & \bar{m}_{k_2,k_2}^{(n)} + e^{-\zeta_{k_2}} & 0 \dots 0 \\ 0 & \dots & 0 & 0 & 1 \dots 0 \\ \vdots & \ddots & \vdots & \vdots & \vdots \ddots \vdots \\ 0 & \dots & 0 & 0 & 0 \dots 1 \end{array} \right| \\
&= e^{-\sum_{s=k_2+1}^{N_2} \zeta_s} \times \left(\left| \begin{array}{ccc} \bar{m}_{1,1}^{(n)} & \dots & \bar{m}_{1,k_2-1}^{(n)} & \bar{m}_{1,k_2}^{(n)} \\ \vdots & \ddots & \vdots & \vdots \\ \bar{m}_{k_2-1,1}^{(n)} & \dots & \bar{m}_{k_2-1,k_2-1}^{(n)} & \bar{m}_{k_2-1,k_2}^{(n)} \\ 0 & \dots & 0 & e^{-\zeta_{k_2}} \end{array} \right| + \left| \begin{array}{ccc} \bar{m}_{1,1}^{(n)} & \dots & \bar{m}_{1,k_2-1}^{(n)} & \bar{m}_{1,k_2}^{(n)} \\ \vdots & \ddots & \vdots & \vdots \\ \bar{m}_{k_2-1,1}^{(n)} & \dots & \bar{m}_{k_2-1,k_2-1}^{(n)} & \bar{m}_{k_2-1,k_2}^{(n)} \\ \bar{m}_{k_2,1}^{(n)} & \dots & \bar{m}_{k_2,k_2-1}^{(n)} & \bar{m}_{k_2,k_2}^{(n)} \end{array} \right| \right), t \rightarrow \infty.
\end{aligned}$$

With Eq. (6) and Lemma 4, one can obtain the result presented in Lemma 2.

Acknowledgments. The research is supported by the National Natural Science Foundation of China (Grant No. 12471239), the Guangdong Basic and Applied Basic Research Foundation (Grant No. 2024A1515013106) and Student Research Cultivation Program of the Institute for Advanced Study, Shenzhen University. The work of TK was supported by DST-SERB, Government of India, in the form of a major research project (File No. EMR/2015/001408). TK also thanks the Principal and Management of Bishop Heber College, Tiruchirappalli, for constant support and encouragement.

[1] Y. S. Kivshar and G. P. Agrawal. *Optical Solitons: From Fibers to Photonic Crystals*. Academic Press, San Diego, 2003.

[2] N. Akhmediev and A. Ankiewicz. *Solitons: Nonlinear Pulses and Beams*. Chapman and Hall, London, 1997.

[3] E. Infeld and G. Rowlands. *Nonlinear Waves, Solitons and Chaos*. Cambridge University Press, Cambridge, 2000.

[4] G. P. Agrawal. *Applications of Nonlinear Fiber Optics*. Academic Press, San Diego, 2001.

[5] G. B. Whitham. *Linear and Nonlinear Waves*. John Wiley & Sons, Inc., New York, 1999.

[6] V. I. Petviashvili and O. A. Pohokotolov. *Solitary Waves in Plasmas and in the Atmosphere*. Routledge, 2016.

[7] P. G. Kevrekidis, D. J. Frantzeskakis, and R. Carretero-González. *Emergent Nonlinear Phenomena in Bose-Einstein Condensates: Theory and Experiment*. Springer Science & Business Media, Berlin, 2007.

[8] P. G. Drazin and R. S. Johnson. *Solitons: An Introduction*. Cambridge University Press, Cambridge, 1989.

[9] Y. S. Kivshar and B. Luther-Davies. Dark optical solitons: Physics and applications. *Physics Reports*, 298(2-3):81–197, 1998.

[10] G. Biondini, D. K. Kraus, B. Prinari, and F. Vitale. Polarization interactions in multi-component defocusing media. *Journal of Physics. A. Mathematical and Theoretical*, 48(39):395202, 2015.

[11] Y. Ohta, D. Wang, and J. Yang. General n-dark-dark solitons in the coupled nonlinear schrödinger equations. *Studies in Applied Mathematics*, 127(4):345–371, 2011.

[12] T. Kanna and M. Lakshmanan. Exact soliton solutions, shape changing collisions, and partially coherent solitons in coupled nonlinear schrödinger equations. *Physical Review Letters*, 86(22):5043–5046, 2001.

[13] S. Stalin, R. Ramakrishnan, M. Senthilvelan, and M. Lakshmanan. Nondegenerate solitons in manakov system. *Physical Review Letters*, 122(4):043901, 2019.

[14] M. J. Ablowitz and P. A. Clarkson. *Solitons, Nonlinear Evolution Equations and Inverse Scattering*. Cambridge University Press, Cambridge, 1991.

- [15] S. Erbay and E. S. Suhubi. Nonlinear wave propagation in micropolar media–i. the general theory. *International Journal of Engineering Science*, 27(8):895–914, 1989.
- [16] M. V. Foursov. Classification of certain integrable coupled potential kdv and modified kdv-type equations. *Journal of Mathematical Physics*, 41(9):6173–6185, 2000.
- [17] M. J. Ablowitz, G. Mussardo, B. Prinari, and A. D. Trubatch. Moving embedded lattice solitons. *Chaos: An Interdisciplinary Journal of Nonlinear Science*, 16(1):013126, 2006.
- [18] H. Leblond and D. Mihalache. Models of few optical cycle solitons beyond the slowly varying envelope approximation. *Physics Reports*, 523(2):61–126, 2013.
- [19] Q. Zha and Z. Li. Darboux transformation and multi-solitons for complex mkdv equation. *Chinese Physics Letters*, 25(2):8–11, 2008.
- [20] Y. Zhang, X. Tao, and S. Xu. The bound-state soliton solutions of the complex modified kdv equation. *Inverse Problems*, 36(6):065003, 2020.
- [21] W. Liu, Y. Zhang, and J. He. Dynamics of the smooth positons of the complex modified kdv equation. *Waves in Random and Complex Media*, 28(2):203–214, 2018.
- [22] Z. Zhang, X. Yang, and B. Li. Soliton molecules and novel smooth positons for the complex modified kdv equation. *Applied Mathematics Letters*, 103:106168, 2020.
- [23] N. Lv and L. Huang. Breather-soliton molecules and breather-positons for the extended complex modified kdv equation. *Communications in Nonlinear Science and Numerical Simulation*, 107:106148, 2022.
- [24] A. Ankiewicz, J. M. Soto-Crespo, and N. Akhmediev. Rogue waves and rational solutions of the hirota equation. *Physical Review E*, 81(4):046602, 2010.
- [25] Q. Zha. Nth-order rogue wave solutions of the complex modified korteweg-de vries equation. *Physica Scripta*, 87(6), 2013.
- [26] J. He, L. Wang, L. Li, K. Porsezian, and R. Erdélyi. Few-cycle optical rogue waves: complex modified korteweg–de vries equation. *Physical Review E*, 89(6):062917, 2014.
- [27] B. Yang and J. Yang. *Rogue Waves in Integrable Systems*. Springer Nature, San Diego, CA, 2024.
- [28] G. Stewart. Long time decay and asymptotics for the complex mkdv equation. *SIAM Journal on Mathematical Analysis*, 57(1):825–885, 2025.
- [29] Y. Y. Ge and Y. R. Wang. Interaction and asymptotic analysis of soliton solutions of the (2+1)-dimensional nonlocal complex mkdv. *Nonlinear Dynamics*, 113(17):23485–23506, 2025.
- [30] W. F. Weng, G. Q. Zhang, and Z. Y. Yan. The focusing complex mkdv equation with nonzero background: Large n -order asymptotics of multi-rational solitons and related painlevé-iii hierarchy. *Journal of Differential Equations*, 415(15):303–364, 2025.
- [31] A. A. Mohammad and M. Can. Exact solutions of the complex modified korteweg - de vries equation. *Journal of Physics A: Mathematical and General*, 28(11):3223–3233, 1995.
- [32] G. Zhang, Z. Yan, and L. Wang. The general coupled hirota equations: modulational instability and higher-order vector rogue wave and multi-dark soliton structures. *Proceedings of the Royal Society A*, 475(2222):20180625, 2019.
- [33] R. Ye, Y. Zhang, and W. Ma. Darboux transformation and dark vector soliton solutions for complex mkdv systems. *Partial Differential Equations in Applied Mathematics*, 4:100161, 2021.
- [34] R. Ye, Y. Zhang, and W. Ma. Bound states of dark solitons in n-coupled complex modified korteweg-de vries equations. *Acta Applicandae Mathematicae*, 178:7, 2022.
- [35] Y. Kodama, V. U. Pierce, and F.-R. Tian. On the whitham equations for the defocusing complex modified kdv equation. *SIAM Journal on Mathematical Analysis*, 40(5):1750–1782, 2008.
- [36] S. Zeng and Y. Liu. The whitham modulation solution of the complex modified kdv equation. *Mathematics*, 11(13):2810, 2023.
- [37] D. Wang, L. Xu, and Z. Xuan. The complete classification of solutions to the riemann problem of the defocusing complex modified kdv equation. *Journal of Nonlinear Science*, 32(1):3, 2022.
- [38] L. Li, C. Duan, and F. Yu. An improved hirota bilinear method and new application for a nonlocal integrable complex modified korteweg-de vries (mkdv) equation. *Physics Letters A*, 383(14):1578–1582, 2019.
- [39] J. Li, J. Chen, and B. Li. Gradient-optimized physics-informed neural networks (gopinns): a deep learning method for solving the complex modified kdv equation. *Nonlinear Dynamics*, 107(1):781–792, 2022.
- [40] R. Hirota. *The Direct Method in Soliton Theory*. Cambridge University Press, Cambridge, 2004.
- [41] M. Sato. Soliton equations as dynamical systems on infinite dimensional grassmann manifolds. *RIMS Kokyuroku*, 439:30–46, 1981.
- [42] M. Jimbo and T. Miwa. Solitons and infinite dimensional lie algebras. *Publ. RIMS, Kyoto Univ.*, 19(3):943–1001, 1983.
- [43] E. Date, M. Jimbo, M. Kashiwara, and T. Miwa. Transformation groups for soliton equations. *Physica D: Nonlinear Phenomena*, 4(3):343–365, 1982.
- [44] Y. Ohta. Dark soliton solution of sasa-satsuma equation. In *AIP Conference Proceedings*, volume 1212, pages 114–121. AIP Publishing, 2010.
- [45] T. Wang, Z. Qin, G. Mu, and F. Zheng. General high-order rogue waves in the hirota equation. *Applied Mathematics Letters*, 140:108571, 2023.